

Removal of phenol from wastewater using fly ash as adsorbent

*Thesis submitted in partial fulfilment of the requirement
for the award of the degree of*

Master of Technology

in

CHEMICAL ENGINEERING

By

MANISH KUMAR DHIMAN

Reg. No: 601211003

Under the Guidance of

Dr. Raj Kumar Gupta
Associate Professor

Dr. Vijaya Kumar Bulasara
Assistant Professor

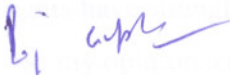


**DEPARTMENT OF CHEMICAL ENGINEERING
THAPAR UNIVERSITY
PATIALA - 147004
PUNJAB, INDIA**

ACKNOWLEDGEMENTS Certificate

This is to certify that the project report entitled "Removal of phenol from wastewater using fly ash as adsorbent" being submitted by **Manish Kumar Dhiman** in partial fulfilment for the requirement of degree of Master of Technology in Chemical Engineering from Thapar University, Patiala is an authentic work done by him under our guidance and supervision.

Date: 14/07/2014



Dr. Raj Kumar Gupta
Associate professor
Department of Chemical Engineering
Engineering
Thapar University, Patiala



Dr. Vijaya Kumar Bulasara
Assistant professor
Department of Chemical
Engineering
Thapar University, Patiala

Countersigned by:



Dr. Rajeev Mehta
Professor & Head
Department of Chemical Engineering
Thapar University, Patiala

Dr. S. K. Mollapatra 15/7
Dean of Academic Affairs
Thapar University, Patiala

(Manish Kumar Dhiman)

ACKNOWLEDGEMENTS

At first, my heartfelt thanks to the almighty for his abundant blessing showered on me throughout this endeavour to complete this successful work of mine. I am thankful to my parents for their great support throughout my life. I would cherish every moment where my parents were so keen and curious to know about the details and progress of my work which boosted my confidence. I express my deep sense of gratitude to them.

My honourable guides **Dr. RAJ KUMAR GUPTA**, and **Dr. VIJAYA KUMAR BULASARA**, Department of Chemical Engineering, Thapar University, Patiala are the persons to whom I will always remain grateful for their excellent guidance, valuable discussions, encouragement, constructive criticism; and their insights have strengthened this study significantly. They gave me a complete freedom to use my opinion, correcting whenever necessary in my dissertation.

I would like to thank our Head of the Department **Dr. RAJIV MEHTA**, who has at all times been very supportive and accommodating.

I would like to thank all the **faculty members of the department of chemical engineering** for encouraging me to write the thesis successfully.

I would like to thank the most senior person, **Dr. P. K. BAJPAI** (Distinguished Professor) for his guidance and blessings.

I would like to thank all my **colleagues** at Thapar University, Patiala who made the time I spent on this thesis work very enjoyable.

Manish
(**Manish Kumar Dhiman**)

ABSTRACT

In comparison with other methods, adsorption process is the best economically feasible method. Activated carbon and several other materials of natural and synthetic origin have been proven as good adsorbents for the treatment of textile wastewater. However, most of these adsorbents are expensive and require several processing steps for preparation as well as for regeneration. Therefore, an attempt has been made to study the performance of fly ash as the adsorbent for removal of phenol from its aqueous solutions. Phenol is one of the most general pollutants in effluents discharged from diverse industries, which result in severe environmental problems because of its toxicity, low biodegradability and ability to build up in plants and tissues, such as fish which live in the lakes; and streams polluted with phenolic compounds have a revolting astonishing flavour and very bad smell.

Fly ash, which is been considered as discard is found to be giving good removal efficiency as far as phenol is concerned. Three different types of fly ash samples were prepared and subjected to SEM analysis, where it showed that the shape and size tend to decrease when the samples were washed and dried and kept in muffle furnace for further heat treatment. All the three samples were studied at the same parameters such as stirring time, pH, stirring speed. Preliminary experiments showed that the best among them was the sample that was washed and dried giving 92% removal when 5 g/L of adsorbent was used. Therefore, the washed fly ash sample after drying was used for all further experiments to study the effect of different process parameters such as solution pH, contact time, stirring speed, adsorbent dosage, phenol concentration and temperature. The percent removal of phenol was found to be the maximum at the solution pH of 7, stirring speed of 400 rpm, contact time of 2 hours. Adsorption capacity decreased with increasing the adsorbent dosage, whereas it increased with increasing the phenol concentration. The optimum adsorbent dosage was found to be 5 g/L for an initial phenol concentration of 50 mg/L. The adsorption capacity decreased with increasing the temperature indicating the exothermic nature of the process. It was observed that the phenol adsorption onto washed fly ash followed pseudo second order kinetics and Freundlich isotherm model.

CONTENTS

Certificate	i
Acknowledgements	ii
Abstract	iii
Contents	iv-v
List of figures	vi-vii
List of Tables	viii
Notations/Abbreviations	ix
CHAPTER 1 : INTRODUCTION	1-4
1.1 Technologies for removal of phenolic compounds	
1.2 Adsorption technique for wastewater treatment	
1.3 Fly ash	
1.3.1 Chemical composition of fly ash	
1.4 Structure of phenol	
CHAPTER 2 : LITERATURE REVIEW	5-14
2.1 Literature review	
2.2 Gaps identified	
CHAPTER 3 : OBJECTIVES	15
3.1 Objectives	
CHAPTER 4 : EXPERIMENTAL METHODOLOGY	16-17
4.1 Preparation of adsorbent	
4.2 Procedure for adsorption experiments	
4.3 Analysis of phenol solution by UV/Vis spectrophotometer	
CHAPTER 5 : RESULTS AND DISCUSSION	18-40

5.1 Morphological analysis by scanning electron microscope (SEM)	
5.1.1 Energy-dispersive X-ray spectroscopy (EDX)	
5.2 Particle size distribution	
5.3 X-ray diffraction (XRD)	
5.4 Determination of λ_{\max} for phenol solution	
5.5 Calibration curve for phenol	
5.6 Calculations	24-32
5.6.1 Effect of stirrer speed and time	
5.6.2 Effect of fly ash dosage	
5.6.2.1 <i>Effect of used fly ash</i>	
5.6.3 Effect of solution pH	
5.6.4 Effect of phenol concentration	
5.6.5 Effect of Temperature	
5.7 Thermodynamic, Kinetic and Equilibrium studies	32-40
5.7.1 Thermodynamics of adsorption	
5.7.2 Adsorption kinetics	
5.7.2.1 <i>Pseudo first order kinetics</i>	
5.7.2.2 <i>Pseudo second-order kinetics</i>	
5.7.2.3 <i>Intra particle diffusion</i>	
5.7.2.4 <i>Equilibrium adsorption isotherm</i>	
CHAPTER 6 : CONCLUSIONS AND FUTURE WORK	41
REFERENCES	42-44

LIST OF FIGURES

Fig. 1	Structure of phenol	4
Fig. 2	SEM image of washed and dried fly ash	18
Fig. 3	EDX image of adsorbent	19
Fig. 4	Particle size distribution of adsorbent(sample 2)	21
Fig. 5	Schematic of X-ray powder diffractometer	22
Fig. 6	X-ray diffraction pattern for fly ash sample	22
Fig. 7	Plot of absorbance versus wavelength for phenol solution	23
Fig. 8	Calibration curve for aqueous phenol solution	24
Fig. 9	Effect of time on percentage removal of phenol at different stirring speeds	27
Fig. 10	Effect of adsorbent dose on percentage removal of phenol	28
Fig. 11	SEM image of used/spent fly ash	29
Fig. 12	Effect of solution pH on percentage phenol removal	30
Fig. 13	Effect of phenol concentration on percentage removal	31
Fig. 14	Effect of temperature on percentage phenol removal	32
Fig. 15	Plot of ΔG° versus temperature	33
Fig. 16	Pseudo first order kinetic model for adsorption of phenol on fly ash	35
Fig. 17	Pseudo second order kinetic model for adsorption of phenol on fly ash	36
Fig. 18	Intra particle diffusion model for the adsorption of phenol on fly ash	37

Fig. 19	Plot of C_e versus C_e/q_e for the estimation of Langmuir isotherm constants	38
Fig. 20	Variation of equilibrium adsorption intensity with initial phenol concentration	38
Fig. 21	Equilibrium isotherm for the adsorption of phenol on fly ash	39

LIST OF TABLES

Table 1	Calculation of percentage removal and adsorption capacity	16
Table 2	Elemental composition of sample 2	19
Table 3	Fine particle percentage of sample 2	20
Table 4	Adsorption capacity at 120 rpm	25
Table 5	Adsorption capacity at 200 rpm	26
Table 6	Adsorption capacity at 300 rpm	26
Table 7	Adsorption capacity at 400 rpm	26
Table 8	Adsorption capacity at different adsorbent dosages	28
Table 9	Adsorption capacity of used fly ash	29
Table 10	Effect of solution pH on adsorption capacity	30
Table 11	Effect of phenol concentration on adsorption capacity	31
Table 12	Effect of temperature on adsorption capacity	32
Table 13	Values of Gibbs free energy(ΔG°) at different temperatures	33
Table 14	Equilibrium parameters for Langmuir and Fruindlich adsorption isotherms	40

NOTATIONS/ABBREVIATIONS

SEM	Scanning electron microscope
EDS	Energy dispersive x- ray
XRD	X- ray diffractometry
C_i	Initial phenol concentration in the solution, mg/L
C_f	Phenol concentration in the solution after adsorption with fly ash, mg/L
C_j	Fly ash loading (adsorbent dosage), g/L
q_t	Amount of phenol adsorbed per unit weight of fly ash, mg/g
ΔG°	Change in Gibbs free energy, J
ΔH°	Change in enthalpy, J
ΔS°	Change in entropy, J K ⁻¹
R	Universal gas constant, J mol ⁻¹ K ⁻¹
Q_e	Equilibrium dye adsorption capacity, mg/g
k₁	Pseudo first –order rate constant, min ⁻¹
k₂	Pseudo second- order rate constant, g.mg ⁻¹ .min ⁻¹
C_e	Liquid phase concentration of adsorbate at equilibrium, mg/L
Q_m	Maximum adsorption capacity of the adsorbent, mg/g
K_L	Equilibrium adsorption constant of the Langmuir isotherm, L/mg
R_L	Equilibrium adsorption intensity
K_F	Freundlich constant, (mg/g). (mg/L) ⁻¹
N	Exponent in Freundlich isotherm equation
R²	Correlation coefficient

The ever increasing environmental awareness in the recent times has led to closer monitoring of quality of water and wastewater. Organic compounds constitute a very large group of pollutants among which phenol, being a basic structural unit for a variety of synthetic organic compounds, wastewater originating from many chemical plants and pesticide and dye manufacturing industries contain this chemical. Wastewater from other industries such as paper and pulp, resin manufacturing, tanning, textile, plastic, rubber, pharmaceutical and petroleum also contain different types of phenols. Natural sources of phenol into the water include decay of vegetation/organic matter etc. Phenol ranks top 50 in production volumes for chemicals produced in the United States. Phenol is used in the production of slimicide, disinfectant, medicinal preparations for sore throat, ointments, ear and nose drops, analgesic rubs, antiseptic etc. Due to its widespread applications, phenol becomes a common contaminant in aqueous streams. Phenols are considered as priority pollutants since they are harmful to organisms even at low concentrations and many have been classified as hazardous pollutants because of their potential harm to human health. Phenol content in drinking water should not exceed 0.002mg/L as per Indian standard. Populations residing near phenol spills, waste disposal sites, or landfill sites may be at risk for higher exposure to phenol than other populations. It is therefore essential to remove phenol from contaminated industrial aqueous streams before discharged into any water body.

1.1 Technologies for removal of phenolic compounds

Among the unit operations in water and wastewater treatment, adsorption technique remains widely preferred due to its simplicity of design and operation. Other conventional processes for removing phenolic compounds include extraction, steam distillation, bacterial and chemical techniques, oxidation with ozone/hydrogen peroxide (Mokrini et al., 1997), ion-exchange (Chan and Fu, 1998), electrochemical oxidation (Poclaro and Palmas, 1997), reverse osmosis (Goncharuk et al., 2002) and photo catalytic degradation (Koyama et al., 1994).

The various disadvantages associated with these techniques are 1) treated effluent quality not satisfactory 2) high cost of operation 3) used of large amount of chemicals

for oxidation processes, ion-exchange etc. becoming source of secondary pollution 4) difficulty in regeneration causing disposal problems. In fact, there is no single process capable of adequate treatment, mainly due to the complex nature of the effluents. Therefore, in practice, a combination of different processes is often used to achieve the desired water quality in the most economical way.

Biodegradation involves the use of microorganisms such as bacteria, yeasts, algae and fungi which can accumulate and degrade different kind of pollutants. However, their application is often restricted because of technical constraints. Biological treatment requires a large land area and is constrained by sensitivity toward diurnal variation as well toxicity of some chemicals and flexibility in design and operation. With current conventional biodegradation processes, biological treatment is incapable of satisfactory phenol removal.

Chemical methods of phenol abatement like coagulation, flocculation, precipitation-flocculation with Fe (II)/Ca(OH)₂, electrokinetic coagulation, conventional oxidation by oxidizing agents are often expensive and although phenols are removed, accumulation of concentrated sludge creates a disposal problem. Secondary pollution problem may also arise due to excessive chemical use. Advanced oxidation process involves the use of very powerful oxidizing agents such as hydroxyl radicals. Although these methods are efficient for the treatment of waters contaminated with pollutants, they are very costly and commercially unattractive.

Physical methods like membrane-filtration is also associated with the disadvantage of membrane fouling and cost of periodic replacement must be included in any analysis of their economic viability. With abundant literature data, liquid-phase adsorption is one of the most popular methods for the removal of pollutants from wastewater since proper design of the adsorption process will produce a high quality treated effluent. It is an attractive alternative for water treatment; especially if the adsorbent is inexpensive it does not require an additional pre-treatment step before application.

1.2 Adsorption technique of water treatment

Adsorption has been found to be superior compared to other techniques in terms of initial cost, flexibility and simplicity of design, ease of operation and insensitivity to toxic pollutants. Moreover, adsorption does not result in the formation of harmful

substances. Adsorption using commercial activated carbon is the most commonly used method due to highly porous nature and high adsorption capacity resulting from high surface area of the activated carbon surface. But due to its high cost and 10–15% loss during thermal regeneration, alternative low cost adsorbents have attracted the attention of several investigators. The present study deals with utilization of low cost adsorbents for adsorption of phenol from aqueous streams. The aim of this work is to study the ability of fly ash to remove phenol from aqueous solutions. This adsorbent was chosen because of its cheapness and abundance. The equilibrium isotherms and the kinetics for this system have to be determined. The importance of such isotherms and kinetic curves lies in developing a model which accurately represents both the obtained results, and could be used for design purposes.

1.3 Fly ash

In an industrial context, fly ash usually refers to ash produced during combustion of coal. Fly ash is generally captured by electrostatic precipitators or other particle filtration equipment before the flue gases reach the chimneys of coal-fired power plants and together with bottom ash removed from the bottom of the furnace is, in this case, jointly known as coal ash. Depending upon the source and makeup of the coal being burned, the components of fly ash vary considerably, but all fly ash includes substantial amounts of silicon dioxide (SiO_2) (both amorphous and crystalline) and calcium oxide (CaO), both being common ingredients in many coal-bearing rock strata. Fly ash, an oxide rich waste product of thermal power plants can be used as raw material for different industries on proper treatment. In India, a little effort has been paid on proper utilisation of fly ash.

1.3.1 Chemical composition of fly ash

Fly ash material solidifies while suspended in the exhaust gases and is collected by electrostatic precipitators or filter bags. Since the particles solidify rapidly while suspended in the exhaust gases, fly ash particles are generally spherical in shape and range in size from 0.5 μm to 300 μm . The major consequence of the rapid cooling is that only few minerals will have time to crystallize and that largely amorphous, quenched glass remains. Nevertheless, some refractory phases in the pulverized coal will not melt (entirely) and remain crystalline. In consequence, fly ash is a heterogeneous material. SiO_2 , Al_2O_3 , Fe_2O_3 and occasionally CaO are the main

chemical components present in fly ashes. The mineralogy of fly ashes is very diverse. The main phases encountered are a glass phase, together with quartz, mullite and the iron oxides; hematite and magnetite. Other phases often identified are cristobalite, anhydrite, lime, periclase, calcite, sylvite, halite, portlandite, rutile and anatase. The Ca-bearing minerals anorthite, gehlenite, akermanite and various calcium silicates and calcium aluminates identical to those found in Portland cement can be identified in Ca-rich fly ashes. The mercury content can reach 1 ppm, but is generally included in the range 0.01 – 1 ppm for bituminous coal. The concentrations of other trace elements vary as well according to the kind of coal combusted to form it. In fact, in the case of bituminous coal, with the notable exception of boron, trace element concentrations are generally similar to trace element concentrations in unpolluted soils.

1.4 Structure of phenol

Phenol is an aromatic organic compound having the molecular formula C_6H_5OH . The simplest of the class is phenol, which is also called carbolic acid. Phenolic compounds are classified as simple phenols or polyphenols based on the number of phenol units in the molecule.

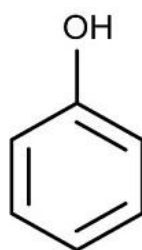


Figure 1: Structure of phenol

2.1 Literature Review

Jain et al. (2004) have utilized blast furnace slag, dust, and sludge from steel plants, as well as carbon slurry from fertilizer plants after treatment as inexpensive adsorbents for the removal of phenols. The characterization of the adsorbents has shown that carbonaceous adsorbent prepared from carbon slurry possesses high porosity and maximum surface area (380 mg/g), compared to those prepared from blast furnace slag, dust, and sludge adsorbents (4–28ml/g). The adsorption of phenols on carbonaceous adsorbent was substantial and found to be 17.2, 50.3, 57.4, and 132.5 mg/g for phenol, 2-CP, 4-CP, and 2,4-DCP, respectively. The adsorption process follows the Langmuir model, first-order, and was pore diffusion controlled. As the adsorption of phenols on prepared carbonaceous adsorbent is significant, its performance has been evaluated with respect to standard activated charcoal. The removal efficiency of phenols using carbonaceous adsorbent was found to be about 45% of that using a standard activated charcoal sample.

Calace et al. (2002) have studied the adsorption of paper mill sludge for phenol, 2-CP, 3-CP, 4-CP, 2-NP, 4-NP, 2,4-DCP, 3,4-DCP, 3,5-DCP, and 2,4,5-TCP. Kinetic experiments showed that adsorption of substituted phenol on paper mill sludge was rapid (equilibrium was reached after 3 h); conversely, the time taken by phenol to reach equilibrium conditions was 260 h. Experimental data showed that particle diffusion was involved in the adsorption process but was not the only rate-limiting mechanism. The adsorption isotherms indicated the following order of retention capacity of paper mill sludge $2\text{-NP} < 4\text{-NP} \ll 2\text{-CP} < \text{phenol} < 4\text{-CP} < 3\text{-CP} < 2,4\text{-DCP} < 3,4\text{-DCP} < 2,4,5\text{-TCP} < 3,5\text{-DCP}$. In all cases, the experimental data showed a good fit with the Hill equation, which is mathematically equivalent to the Langmuir–Freundlich model obtained by assuming that the surface is homogeneous and the adsorption is a cooperative process influenced by solute–solute interactions.

Sathishkumar et al. (2007) have also investigated the removal of 2,4-DCP from aqueous solutions on palm pith carbon under varying conditions such as agitation time, adsorbent dosage, pH, and temperature. More 2,4-DCP was removed with decreasing initial concentration of 2,4-DCP and increasing adsorbent dosage.

Kinetic studies showed that the adsorption of 2,4-DCP on palm pith carbon was a gradual process. Adsorption capacity of 2,4-DCP was 19.2 mg/g for the particle size of 0.25–0.5 mm. Acidic pH was favourable for the adsorption of 2,4-DCP. Studies on pH effect and desorption showed that chemical adsorption seemed to play a major role in the adsorption process. In the adsorption of 2,4-DCP on palm pith carbon, the changes in entropy and enthalpy were estimated to be 30.7 J/(mol.K) and 7.2 kJ/mol, respectively. The highly positive change in Gibbs free energy indicated the feasible and spontaneous adsorption of 2,4-DCP on palm pith carbon.

Juang et al. (2002) have also studied the equilibrium and kinetic of the adsorption of phenol, 3-NP, and o-cresol from water on montmorillonite modified with CTAB. The adsorption capacity decreased in the order phenol > 2-cresol > 3-NP. The Langmuir, dual-mode adsorption, and Redlich–Peterson models were tested to fit the isotherms of single solute systems, whereas the Langmuir competitive model was used to describe bisolute equilibria. Huang et al. (2007) have studied the removal of phenol using octadecyl trimethylammonium chloride (OTMAC)-modified attapulgite from aqueous solutions. The comparison of natural attapulgite and modified attapulgite showed that it is possible to utilize the sonication-modified OTMAC-attapulgite in the treatment of phenol-polluted water. The adsorption kinetics was described by a pseudo-second-order model. The Freundlich model was found to be applicable for describing the equilibrium data.

Yapar et al. (2005) have studied the effect of adsorbent dosage on the adsorption of phenol by hexadecyltrimethylammonium bromide (HDTMAB)-modified bentonite. Experiments were conducted in two stages. The adsorption of HDTMAB on bentonite was studied in the first group of experiments. It was found that all the HDTMAB was adsorbed by bentonite, even when the amount used exceeded 100% of CEC. After the modification of bentonite by HDTMAB in an amount equivalent to 100% of CEC, adsorption experiments were performed at different adsorbent dosages ranging from 2 to 10 g/L. A type V isotherm and a nonlinear increase in percent removal with adsorbent dosage were observed. The nonlinear relationship between the percent removal and adsorbent dosage was due to the effect of intraparticle interactions, and it was represented by a second-order polynomial. Although the Freundlich equation fitted well, it failed to represent the

plateau and the second region that appeared in the isotherm. Hence, an equation correlating the equilibrium concentration and initial and adsorbent concentrations was suggested.

Srivastava et al. (2006) have studied the adsorption of phenol on carbon rich bagasse fly ash (BFA). Optimum conditions for phenol removal were found to be pH 6.5, adsorbent dosage 10 g/L of solution, and equilibrium time 5 h. Adsorption of phenol followed the pseudo-second-order kinetics with the initial rate on laboratory-grade activated carbon being the highest, followed by those on BFA and commercial-grade activated carbon. The Redlich–Peterson isotherm was found to best represent the data for phenol adsorption on all the adsorbents. The change in entropy and enthalpy for phenol adsorption on BFA was 169 J/(mol K) and 47 kJ/mol, respectively. The highly negative change in Gibbs free energy indicated the spontaneous adsorption of phenol on BFA.

Erso et al. (2004) have also investigated the removal of phenols with a NP-imprinted polymer from water by a newly functional monomer, methacrylamidoantipyrine (MAAP). The adsorption capacity for NP and other phenols on molecularly imprinted polymers (MIPs) significantly depend on the use of functional monomers. The maximum adsorption of NP on MIP beads was 24.1 mg/g for MAAP and 13.5 mg/g for MAAP-based imprinted polymers. Furthermore, the pH significantly affected the adsorption capacity of MIPs. The hyper-crosslinked polystyrene beads with bimodal pore size distribution were prepared through the Friedel-Crafts modification using macroreticular poly(vinylbenzylchloride-DVB) copolymer beads as base polymers (Oh et al., 2003). Their adsorption behaviours were examined with aqueous solutions of phenol, 4-CP, and 2,4-DCP. The biporous hyper-crosslinked beads gave not only faster adsorption kinetics than commercial polystyrene adsorbents, but also larger adsorption capacity

Abburri et al. (2003) has studied the removal of phenol and 4-CP from synthetic single and bisolute aqueous solutions at 30°C through the adsorption on Amberlite XAD-16 resin under batch equilibrium and dynamic column conditions. The equilibrium data from single component solutions were fitted to the Langmuir and Freundlich models to evaluate the model parameters, and the parameters in turn were used to predict the extent of adsorption from bisolute aqueous solutions using

the ideal solution adsorption model. The effects of pH on the removal of phenol and 4-CP from single and bisolute systems were also studied. The breakthrough capacity and total capacity of the resin for the solutes at different concentrations were evaluated through column studies. Attempts were made to regenerate the resin by solvent washing using methanol. The limited number of adsorption–desorption cycles indicated that the adsorption capacity of the resin remained unchanged.

Radhika and Palanivelu (2006) have studied the adsorptive removal of 4-CP and 2,4,6-TCP from aqueous solutions by activated carbons prepared from coconut shell, and compared with commercial-grade activated carbons (CAC). Various chemical agents at different concentrations (KOH, NaOH, CaCO₃, H₃PO₄, and ZnCl₂) were used for preparing coconut-shell activated carbon (CSAC). The CSAC prepared using KOH as chemical agent showed high surface area and best adsorption capacity and was chosen for further studies. It was found that the Freundlich isotherms best fitted the data for the adsorption of 4-CP and 2,4,6-TCP.

Mukherjee et al. (2007) have studied three carbonaceous materials, activated carbon (AC), bagasse ash (BA), and wood charcoal (WC), as the adsorbents for removing phenol from water. Approximately 98%, 90%, and 90% removal efficiency was achieved for phenol-AC, phenol-WC, and phenol-BA adsorption systems at given conditions. Experimental studies indicated that phenol removal with the selected adsorbents is a first-order adsorption and the Freundlich model well fitted the data for the adsorption of phenol.

Gonzalez-Serrano et al. (2004) have studied the adsorption of phenols by activated carbons prepared from pyrolysis of H₃PO₄-impregnated lignin precipitated from Kraft black liquors. The applications of these carbons for removing pollutants were evaluated by measuring the adsorption capacities for phenol, 2,4,5-TCP and Cr(VI) as the representatives of toxic contaminants. An impregnation ratio and an activation temperature of 2 g H₃PO₄/g lignin and 430°C, respectively, are recommended as the best combination of operating conditions to prepare carbons for aqueous-phase applications. Dried and crushed corncobs were carbonized at 500°C and steam activated (in one- or two-step scheme), or activated with H₃PO₄ (El-Hendawy et al., 2001). Adsorption capacity was demonstrated by the iodine and phenol numbers, and the isotherms of methylene blue and Pb, from aqueous solutions.

Enhanced porosity was best associated with chemical activation. Phenol uptake was found to depend on surface chemical nature of the carbon rather than its porous properties. Corncobs were postulated to be feasible as feed stock to produce good adsorbing carbons, under one-step activation scheme outlined here.

Tor et al. (2006) have studied the adsorption of phenol with red mud as functions of contact time, pH, initial phenol concentration, red mud dosage, and effect of salt addition. Experimental results demonstrated that the maximum phenol removal was obtained in a wide pH range of 1.0– 9.0 and it took 10 h to attain equilibrium. The isotherm data were analyzed using the Langmuir and Freundlich models, and it was found that the latter represented the measured data better. The influence of added salt on phenol removal depends on the relative affinity of the anions for red mud surface and the relative concentrations of the anions.

Sarkar and Acharya (2006) have studied the removal of phenol and its analogy from water with CFA. The equilibrium data was best fitted by the Langmuir model. The process was endothermic and thermodynamically spontaneous in nature. The positive value of entropy change suggested the increased randomness. The use of CFA as an adsorbent for phenolic compounds was found to be cost effective and thus can be considered as an alternative to activated carbon. The leaching test carried out with water indicated that the disposal of CFA did not pose any extra load of phenolic compounds to the landfill, as no release of phenols from CFA bed occurs. Moreover, phenolic compounds can be recycled and utilized as industrial raw materials as they can be recovered quantitatively from the CFA bed.

Otero et al. (2003) have used the adsorbents produced from sewage sludge in organic pollutant removal. After chemical activation and pyrolysis treatment, sewage sludge provided materials of great porosity and high surface area. The properties of this type of material were studied by liquid-phase adsorption using crystal violet, indigo carmine, and phenol as the solutes. It is found that activated carbons prepared from sewage sludge were promising for this purpose.

Adak et al. (2006) have indicated alumina to be a very efficient adsorbent for the removal of anionic surfactant from highly concentrated wastewater. After the removal of surfactant in several cycles, the exhausted surfactant-coated alumina

becomes useless. This exhausted alumina, however, possess the ability to remove organics from aquatic environment through the process called solubilization. In their study, the exhausted alumina, hereafter designated as surfactant (sodium dodecyl sulfate, SDS)-modified alumina (SMA), was used for adsorptive removal of phenol from water. It was found that the removal followed the second-order kinetics. Studies were conducted to see the effect of SMA dosage on the removal of phenol. The pH was maintained at 6.7. SMA was found to be very efficient and 90% efficiency could be achieved under optimized conditions for the removal of phenol from phenol-spiked distilled water. Desorption of both SDS and phenol from the SMA surface was possible using 0.25 M NaOH solutions. Desorption of phenol only is also possible by acetone or rectified spirit.

Roostaei and Tezel (2004) have examined the liquid-phase adsorption of phenol from water by silica gel, HiSiv 3000, activated alumina, activated carbon, Filtrasorb-400, and HiSiv 1000. The Langmuir–Freundlich type of isotherm model was the best to describe adsorption equilibrium data for phenol for all the adsorbents studied. Kinetic results indicated that HiSiv 1000 had the highest adsorption rate among the adsorbents. The effects of particle size, temperature, and thermal regeneration on the adsorption of phenol by HiSiv 1000 were evaluated. It was found that adsorption capacity decreased with increasing temperature. Thermal regeneration of HiSiv 1000 was performed at 360°C. It was observed that adsorption capacity of HiSiv 1000 did not change after 14 regeneration cycles. Equilibrium experiments showed that the adsorption capacities of activated carbon and Filtrasorb-400 were several times higher than that of HiSiv 1000. Removal of phenolic compounds from industrial wastewater was studied by adsorption in fixed-bed with polymeric resins

Tarasevich et al. (2001) has shown that natural long-flame coal from the Donbas field has well developed micro and mesoporous structure and may adsorb a wide range of organic compounds from water. This property, along with its low-cost, makes this coal a promising material for the purification of natural and wastewaters.

Parida (2009) have studied the Adsorption of phenol on water washed manganese nodule leached residue (WMNLR), waste materials from manganese nodules processing plant. The increase in percentage of adsorption with increase in temperature indicates that adsorption is endothermic in nature. The pseudo-second-

order kinetics was followed in the adsorption process. The thermodynamic study reveals that adsorption is a spontaneous and endothermic process. A maximum loading capacity of 28.5 mg/g was observed at an adsorbent dose of 1.0 g/L, phenol concentration 30 mg/L and 4 h equilibrium time.

Muthamil et al. (2012) developed a pongamia glabra flower (PGF) adsorbent and tested for its ability to remove phenol in aqueous solution. Adsorption studies were performed in a batch system, and effects of various experimental parameters such as solution pH, contact time, initial phenol concentration, adsorbent concentration and temperature were evaluated upon the phenol adsorption onto PGF. Maximum phenol removal was observed at pH 6 equilibrium was attained after contact of 6 h only. The adsorption isotherms were in conformation to both Langmuir and Freundlich isotherm models. The kinetics studies indicated that the adsorption process was best described by the pseudo-second-order kinetics.

Cornelia et al. (2013) prepared and studied two new poly (styrene-co-divinylbenzene) polymers functionalized with amino-phosphinic acid groups (P1) and with carboxylic acid groups (P2) and their adsorption capacities for phenol and p-chloro phenol (PCP) in aqueous solutions were investigated. The kinetics studies demonstrated that the adsorption of phenol and PCP onto P1, P2 and XAD-4 adsorbents followed the pseudo-second order model. The experimental equilibrium data were fitted with Langmuir, Freundlich, Redlich–Peterson, and Sips isotherms. P2 polymer showed the best adsorption capacity. These results suggest the potential application of the P2 resin for the removal of phenolic pollutants from wastewaters.

Sharma et al. (2005) investigated the possible use of coal, residual coal, and residual coal treated with H_3PO_4 as a means of removal of phenol from wastewater. The study was realized using batch experiments, with synthetic wastewater having phenol concentration of 1000 ppm. Other low-cost adsorbents such as petroleum coke, coke breeze, rice husk, and rice husk char have also been used. The effect of system variables such as pH, contact time, and temperature has been investigated. The suitability of the Freundlich, Langmuir, and Redlich–Peterson adsorption models to the equilibrium data was investigated for each phenol–adsorbent system. The results showed that the equilibrium data for all the phenol–sorbent systems fitted the Redlich–Peterson model best.

Su hisa lin et al. (2008) the technical feasibility of the use of activated carbon, synthetic resins, and various low cost natural adsorbents for the removal of phenol and its derivatives from contaminated water has been reviewed. Instead of using commercial activated carbon and synthetic resins, researchers have worked on inexpensive materials such as coal fly ash, sludge, biomass, zeolites, and other adsorbents, which have high adsorption capacity and are locally available. The comparison of their removal performance with that of activated carbon and synthetic resins is presented in this study. From our survey of about 100 papers, low-cost adsorbents have demonstrated outstanding removal capabilities for phenol and its derivatives compared to activated carbons. Adsorbents that stand out for high adsorption capacities are coal-reject, residual coal treated with H_3PO_4 , dried activated sludge, red mud, and cetyltrimethylammonium bromide-modified montmorillonite.

Gupta and Suhas (2009) provided an overview of the application of low-cost adsorbents comprising natural, industrial as well as synthetic materials/wastes and their application for dyes removal.

Uma et al. (2009) evaluated the adsorptive characteristics of rice husk ash as an effective adsorbent for Indigo Carmine dye. Their study explored the adsorptive characteristics of Indigo Carmine (IC) dye from aqueous solution onto rice husk ash. Batch experiments were carried out to determine the influence of parameters like initial pH, contact time (t), adsorbent dose (m) and initial concentration on the removal of IC. The optimum conditions were found to be: $pH_0 = 5.4$, $t = 8$ h and $m = 10.0$ g/l. The pseudo-second-order kinetic model represented the adsorption kinetics of IC on to RHA. Equilibrium isotherms were analyzed by Freundlich, Langmuir, Temkin and Redlich Peterson models using a non-linear regression technique.

Maria et al. (2006) studied the characterization of an adsorbent prepared from maize waste and adsorption of three classes of textile dyes. They were investigated and accomplished in order to evaluate both inexpensive and alternative materials as potential adsorbents for pollutants and coloured compounds. A novel adsorbent, prepared from maize waste, was activated and characterized under the aspect of its reproducible employment using elemental analysis, thermogravimetry, porosimetry and adsorption of different dyes from solution.

Crini (2006) presented a review on the non-conventional low-cost adsorbents for dye removal. Adsorption techniques are widely used to remove certain classes of pollutants from waters, especially those that are not easily biodegradable. Dyes represent one of the problematic groups. Currently, a combination of biological treatment and adsorption on activated carbon is becoming more common for removal of dyes from wastewater. Although commercial activated carbon is a preferred sorbent for colour removal, its widespread use is restricted due to high cost. As such, alternative non-conventional sorbents have been investigated. It is well-known that natural materials, waste materials from industry and agriculture and biosorbents can be obtained and employed as inexpensive sorbents.

Anna et al. (2011) studied the biosorption of heavy metals from aqueous solutions onto peanut shell as a low-cost biosorbent. They were performed biosorption of Cu(II) and Cr(III) ions from aqueous solutions by peanut shell biomass was investigated as a function of initial pH, initial biomass concentration and temperature. The optimum sorption conditions were studied for each metal separately. The kinetics and equilibrium of biosorption were examined in detail. Four kinetic models (pseudo-first order, pseudo second order, power function equation, and Elovich model) were used to correlate the experimental data and to determine the kinetic parameters. Four well-known adsorption isotherms were chosen to describe the biosorption equilibrium. The experimental data were analyzed using two two-parameter models (Langmuir and Freundlich) and two three parameter models (Redlich–Peterson and Sips). The equilibrium biosorption isotherms showed that peanut shells possess high affinity and sorption capacity for Cu (II) and Cr (III) ions, with monolayer sorption capacities of 25.39 mg Cu²⁺ and 27.86 mg Cr³⁺ per 1 g biomass, respectively. All results showed that peanut shells biomass is an attractive, alternative low-cost biosorbent for removal of heavy metal ions from aqueous media.

2.2 Gaps identified

A thorough review of the existing literature indicated that several natural and synthetic adsorbents have been studied for the removal of phenol and phenolic compounds from their aqueous solutions. However, coal fly ash has not been studied for the adsorption of phenols. Since fly ash is cheap and abundant, there is a substantial scope for utilizing this industrial waste as a potential adsorbent for the

removal of phenol and its derivatives. Therefore, exploring the adsorption potential of fly ash for the removal of phenol has been considered in this work.

3.1 Objectives

The main objective is to explore the adsorption potential of coal fly ash for the removal of phenol from its aqueous solutions. The specific objectives of the present investigation are as follows.

- Characterization of fly ash by XRD, SEM/EDAX and PSD (particle size distribution)
- To identify best sample of fly ash for removal among three samples
- To carry out adsorption experiments and to study the effects of initial dye concentration, contact time, fly ash dosage, stirring speed, pH and temperature for the adsorption of phenol over fly ash in batch mode
- Thermodynamic study of adsorption
- To study the adsorption kinetics using various kinetic models

4.1 Preparation of adsorbent

- Raw fly ash is taken from thermal plant, Ropar and is labeled as **Sample 1**.
- Fly ash is washed in water and dried. It is labeled as **Sample 2**.
- Fly ash is washed, dried and kept in muffle furnace for 5 hours at 550°C. It is labeled as **Sample 3**.

After performing the removal percentage experiments, as shown in Table 1 for different adsorbents, it was found that sample 2 shows higher removal efficiency because unburnt carbon in fly ash played a key role in the removal of phenol. Therefore, sample 2 was selected and used in all further experiments to study the effect of different operating parameters. Initially 50 ppm concentration of phenol was taken in all the experiments.

Table 1: Calculation of removal efficiency and adsorption capacity

Adsorbent Sample no.	Concentration of adsorbent (gm/L)	Stirring speed (rpm)	pH	Final concentration (ppm)	% Removal	Adsorption capacity (mg/g)
1	1	120	7.0	49	2	1
2	1	120	7.0	47	6	3
3	1	120	7.0	48	4	2
1	5	120	7.0	20	60	6
2	5	120	7.0	4	92	9.2
3	5	120	7.0	10	80	8

4.2 Procedure for adsorption experiments

Procedure for adsorption experiments for the removal of phenol using fly ash consist of following steps.

- A 100 ml of standard phenol solution (50 mg/L) is freshly prepared by mixing the required amount of phenol in distilled water in a 250 ml beaker.

- ii) The pH of the solution is checked and adjusted to desired value by adding a few drops of standard HCL/NaOH solution.
- iii) A desired amount of fly ash is then added into the beaker containing the phenol and it is well mixed.
- iv) Adsorption is carried out for desired time under continuous agitation at desired speed.
- v) Fly ash is then allowed for 30 min. to settle down and the solution is carefully separated from the fly ash.
- vi) The collected sample is then analyzed by UV-Visible spectrophotometer and the absorbance value is noted down.
- vii) These absorbance values are matched with the corresponding calibration curve to obtain the phenol concentration in the solution after adsorption with fly ash.
- viii) Phenol removal percentage and the adsorption capacity of the fly ash are calculated using equations (2) and (3).

4.3 Analysis of phenol solution by UV/Vis spectrophotometer

UV/Vis refers to absorption spectroscopy or reflectance spectroscopy in the ultraviolet-visible spectral region. This means it uses light in the visible and adjacent (near-UV and near-infrared) ranges. The absorption or reflectance in the visible range directly affects the perceived colour of the chemicals involved. In this region of the electromagnetic spectrum, molecules undergo electronic transitions. This technique is complementary to fluorescence spectroscopy, in that fluorescence deals with transitions from the excited state to the ground state, while absorption measures transitions from the ground state to the excited state. They can be designed to measure the absorbance on any of the listed light ranges that usually cover around 200-2500 nm using different controls and calibration. Within these ranges of light, calibrations are needed on the machine using standards that vary in type depending on the wavelength of the photometric determination. The position of the maximum absorbance of phenol solution was determined to be at 293 nm on a spectrophotometer.

5.1 Morphological analysis by scanning electron microscope (SEM)

A scanning electron microscope (SEM) (Joel, JSM 5800) is a type of electron microscope that produces images of a sample by scanning it with a focused beam of electrons. The electrons interact with atoms in the sample, producing various signals that can be detected and that contain information about the sample's surface topography and composition. The electron beam is generally scanned in a raster scan pattern, and the beam's position is combined with the detected signal to produce an image.

Figure 2 shows that most of the particles present in the fly ash are spherical in shape with a relatively smooth surface.

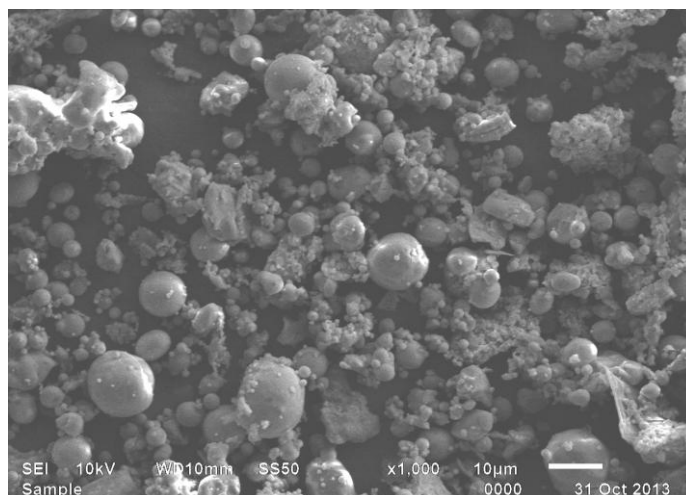


Figure 2: SEM image of washed and dried fly ash (sample 2)

5.1.1 Energy-dispersive X-ray spectroscopy (EDX)

It is an analytical technique used for the elemental analysis or chemical characterization of a sample. It relies on the investigation of an interaction of some source of X-ray excitation and a sample. Its characterization capabilities are due in large part to the fundamental principle that each element has a unique atomic structure allowing unique set of peaks on its X-ray spectrum. To stimulate the emission of characteristic X-rays from a specimen, a high-energy beam of charged particles such as electrons or protons or a beam of X-rays, is focused into the sample

being studied. At rest, an atom within the sample contains ground state (or unexcited) electrons in discrete energy levels or electron shells bound to the nucleus. The incident beam may excite an electron in an inner shell, ejecting it from the shell while creating an electron hole where the electron was. An electron from an outer, higher-energy shell then fills the hole, and the difference in energy between the higher-energy shell and the lower energy shell may be released in the form of an X-ray. The number and energy of the X-rays emitted from a specimen can be measured by an energy-dispersive spectrometer. As the energy of the X-rays are characteristic of the difference in energy between the two shells, and of the atomic structure of the element from which they were emitted, this allows the elemental composition of the specimen to be measured. Table 2 shows the elemental composition of the three fly ash samples determined by EDX analysis. Corresponding figures of EDX analysis are shown in Figure 3

Table 2: Elemental composition of sample 2

Element	Sample 2	
	Weight %	Atomic %
Si	45.94	52.65
Al	33.15	39.55
Zr	20.02	7.06
K	0.89	0.73

Silicon and aluminum are the major components in the fly ash. A small amount of zirconium is also present.

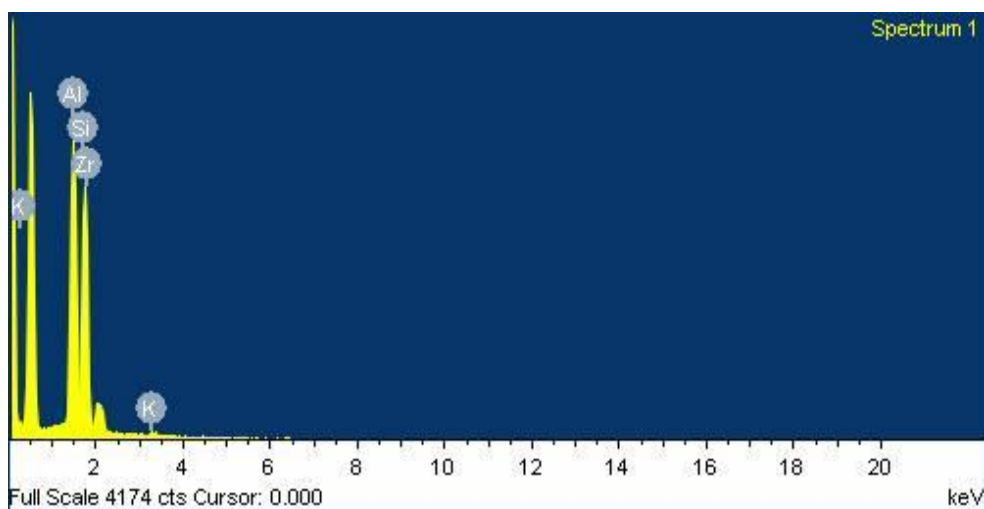


Figure 3: EDX image of adsorbent (sample 2)

5.2 Particle size distribution

The particle-size distribution (PSD) (Malvern instruments M7) of a powder, or granular material, or particles dispersed in fluid, is a list of values or a mathematical function that defines the relative amount, typically by mass, of particles present according to size. PSD is also known as grain size distribution. PSD is usually defined by the method by which it is determined. The most easily understood method of determination is sieve analysis, where powder is separated on sieves of different sizes. This continues to be used for many measurements because of its simplicity, cheapness, and ease of interpretation. Methods may be simple shaking of the sample in sieves until the amount retained becomes more or less constant. The data obtained is shown in Table 3 and Figure 4.

Table 3: Fine particle percentage of sample 2

Particle Size (μm)	Fine Particle %
2000	99.48
1700	98.84
1000	98.28
710	97.64
500	96.86
355	96.02
250	87.98
150	45.30
106	32.92
75	13.16
53	3.30

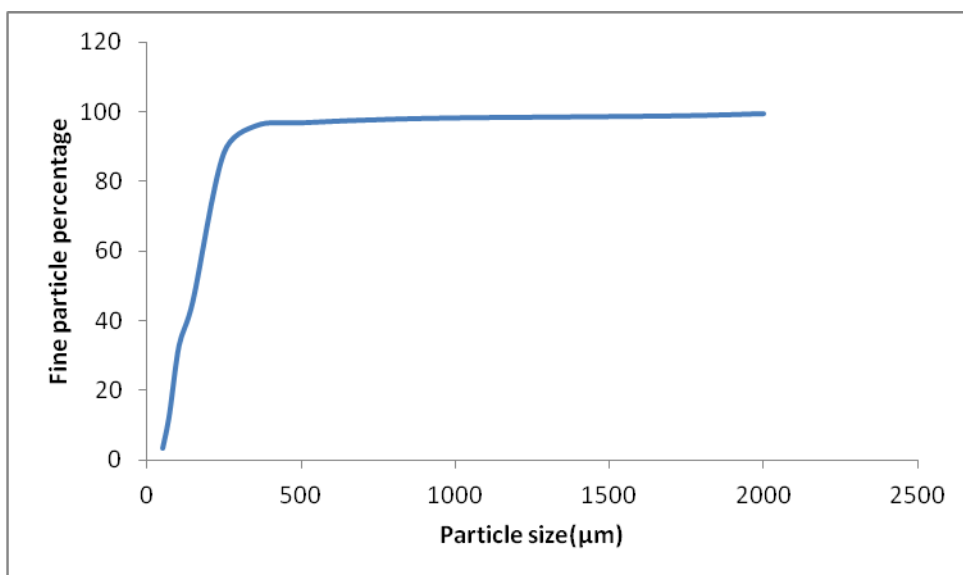


Figure 4: Particle size distribution of adsorbent (sample 2)

5.3 X-ray diffraction (XRD)

As prepared sample was characterized by XRD diffractometer with CuK_α radiation for the identification of existing phases and their volume fractions, crystal structure, lattice parameter of the crystalline solids. i.e. how the atoms pack together in the crystalline state and what the interatomic distance and angle are etc. The sample is irradiated with monochromatic x-rays and the counters record the reflected radiation (shown in Figure 5). In this technique, various forms of the samples could be tested and small amount is required for phase determination. The X-ray diffraction patterns were recorded using Bruker's diffractogram with CuK_α radiation ($\lambda = 1.5418 \text{ \AA}$) obtained from copper target using an in built Ni filter.

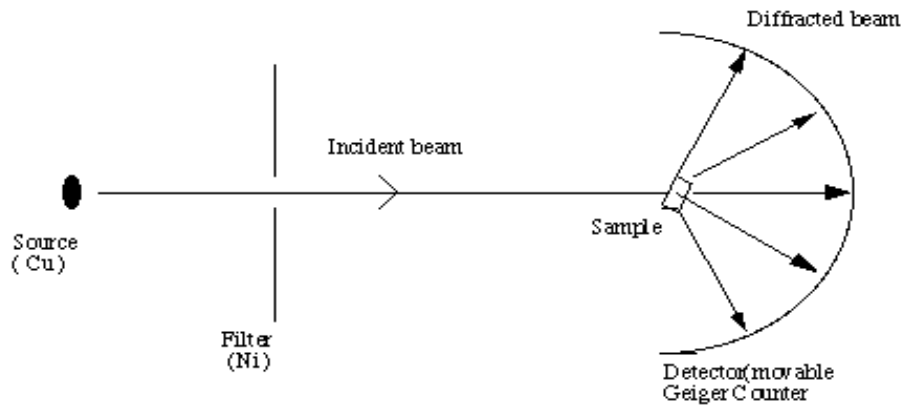


Figure 5: Schematic of X-ray powder diffractometer

The 2θ values for XRD patterns, in the range of 10° to 90° are sufficient to cover the most useful part of the powder pattern. The interplanar spacing (d) values of samples were calculated using the Bragg's law.

$$2d \sin \theta = n \lambda \quad (1)$$

Where, λ is the wavelength of incident X-ray, d is the interplanar distance and θ is diffraction angle. The XRD patterns were identified using powder diffraction files (PDF). Figure 6 shows the X-ray diffraction pattern of the fly ash sample.

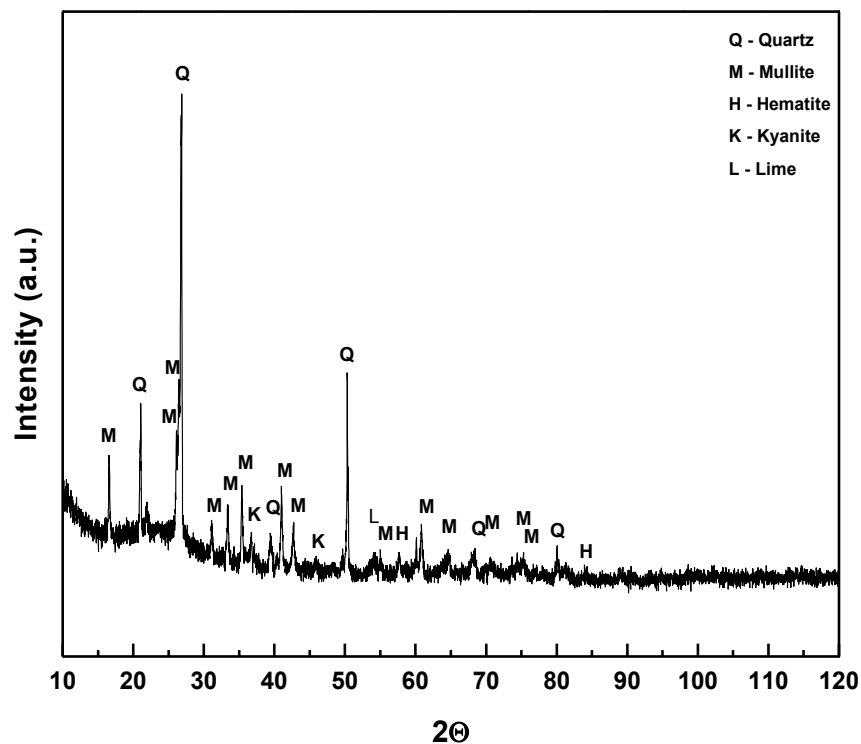


Figure 6: X-Ray diffraction pattern for fly ash sample

Celik et.al, 2008 characterized the fly ash material and studied its effect on the compressive properties of Portland cement also they studied the percentage of oxides present in their fly ash material consisting of SiO_2 (22- 57 %), Al_2O_3 (5.9 – 23.2 %) and Fe_2O_3 (3.6 – 9.8 %). From our XRD measurements, it is concluded that the fly ash material has the oxides such as quartz (Q) (JCPDS card no. 01-082-0511), mullite (M) (JCPDS card no. 00-006-0258), hematite (H) (JCPDS card no. 01-087-1165), kyanite (K) (JCPDS card no. 00-010-0457) and lime (L) (JCPDS card no. 00-82-1690) can be observed. The major portion of fly ash material consists of mullite (45.5%), quartz (42.5%), kyanite (5.5%), hematite (4.3%) and lime (2.2%).

5.4 Determination of λ_{max} for phenol solution

To determine the wavelength that corresponds to maximum absorbance (λ_{max}), a standard solution of phenol in distilled water was scanned through a wavelength range of 200–700 nm using a UV–Visible spectrophotometer. Maximum absorbance value was noticed at a wavelength of 293 nm (Figure 7). Therefore, λ_{max} for phenol was taken as 293 nm. Absorbance values were determined at various known concentrations of the phenol solution to obtain a calibration curve for phenol solution.

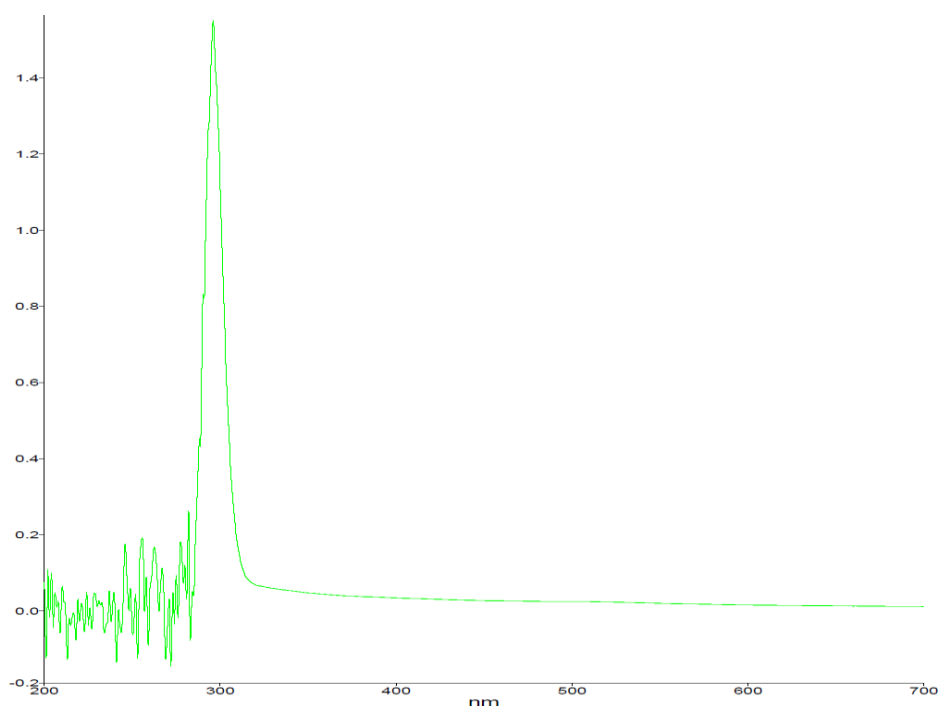


Figure 7: Plot of absorbance versus wavelength for dye solution

5.5 Calibration curve for phenol

Absorbance values were determined at various known concentrations of the phenol solution to obtain a calibration curve for phenol solution. As shown in Figure 8, a linear fit to the observed data (absorbance versus phenol concentration) yielded a straight line with a slope of 0.3102. This calibration curve can be used for the determination of unknown phenol concentration in the solution after adsorption with fly ash.

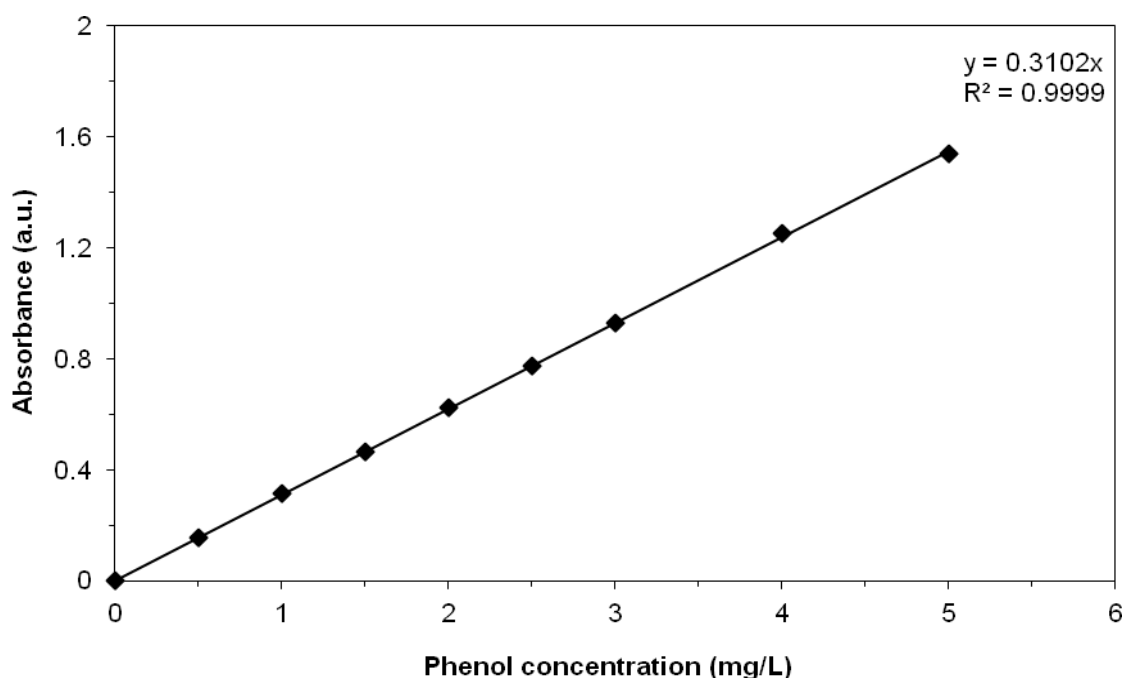


Figure 8: Calibration curve for aqueous phenol solution

5.6 Calculations

Percentage removal of phenol is calculated using the following relation.

$$\% \text{ Removal, } R = \left(\frac{C_i - C_f}{C_i} \right) \times 100 \quad (2)$$

Adsorption capacity (q) is given by the relation;

$$\text{Adsorption capacity, } q = \frac{C_i - C_f}{C_a} \quad (3)$$

Where,

C_i – initial concentration of phenol (mg/L)

C_f – final concentration of phenol (mg/L)

C_a – concentration of the adsorbent (g/L)

5.6.1 Effect of stirrer speed and time

Stirring is an important parameter in adsorption phenomena, influencing the distribution of the solute in the bulk solution and the formation of the external boundary film. To study the effect of stirrer speed on the percentage phenol removal, adsorption experiments were conducted at various stirrer speeds between 100 and 400 rpm. The values of percentage phenol removal for various stirrer speeds are presented in Table 4 to 7 and the corresponding plot of percentage phenol removal versus stirrer speed is shown in Figure 9.

- Impeller diameter: 2.5 cm
- Impeller type: blade type

To study the effect of adsorption time on the percentage phenol removal, phenol concentration values were noted at various time intervals between 0.5 and 6 hours for phenol. The values of percentage phenol removal at various time intervals are presented in Tables 4 to 7 and the corresponding plot of percentage phenol removal versus adsorption time is shown in Figure 9. From this figures, it can be observed that the percentage removal increases with increasing the time of adsorption. The slope of the curve in Figure 9 is decreasing with time, indicating that the adsorption rate is faster initially and it decreases with time as more amount of phenol is adsorbed on the fly ash surface decreasing the availability of active adsorption sites. In all these experiments initial phenol concentration was taken as 50 ppm.

Table 4: Adsorption capacity at 120 rpm

Time (hours)	Final concentration (ppm)	% Removal	Adsorption capacity (mg/g)
0.5	25.17	49.641	4.96
1	15.75	68.532	6.85
2	8.45	83.171	8.31
4	3.95	92.154	9.21
6	1.93	96.144	9.61

Table 5: Adsorption capacity at 200 rpm

Time (hours)	Final concentration (ppm)	% Removal	Adsorption capacity (mg/g)
0.5	23.9	52.2	5.22
1	14.3	71.4	7.14
2	6.35	87.3	8.73
4	2.45	95.12	9.51
6	1.9	96.21	9.62

Table 6: Adsorption capacity at 300 rpm

Time (hours)	Final concentration (ppm)	% Removal	Adsorption capacity (mg/g)
0.5	21.94	56.12	5.6
1	12.43	75.14	7.5
2	4.55	90.9	9.09
4	1.75	96.5	9.65
6	0.7	98.6	9.8

Table 7: Adsorption capacity at 400 rpm

Time (hours)	Final concentration (ppm)	% Removal	Adsorption capacity(mg/g)
0.5	21.0	58.2	5.8
1	10.45	79.1	7.9
2	4	92.0	9.2
4	1.95	96.1	9.6
6	0.6	98.8	9.8

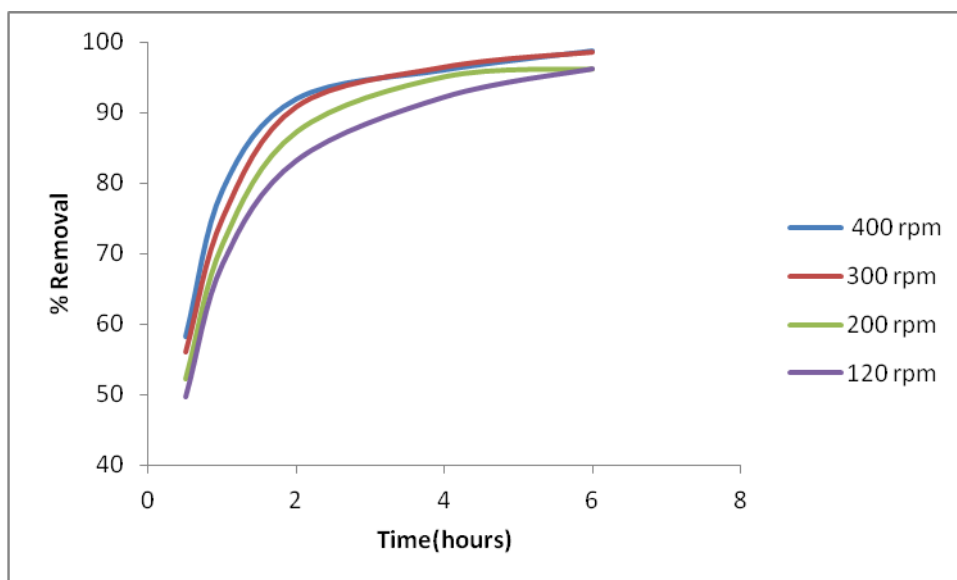


Figure 9: Effect of time on percentage removal of phenol at different stirring speeds

From Figure 9, it is clear that with increasing the agitation speed from 120 to 400 rpm, the percentage removal increased significantly. This can be explained by the fact that increasing agitation speed reduced the film boundary layer surrounding particles, thus increasing the external film transfer coefficient, and hence the adsorption capacity. The degree of agitation reduces the boundary layer resistance and increases the mobility of the system. With agitation, the external mass transfer coefficient increases resulting in quicker adsorption of the phenol molecules. It can be observed from the Figure 9 that agitation could improve the adsorption rate significantly. Very low values of percentage phenol removal were obtained at low stirrer speeds and the percentage removal increased with increasing the stirrer speed. There was no significant variation in percentage removal values at higher stirrer speeds and hence, a stirrer speed of 400 rpm was chosen for the phenol.

5.6.2 Effect of fly ash dosage

The values of percentage phenol removal and adsorption capacity of fly ash evaluated using the formulae (equations 2 and 3) for various concentration of fly ash are listed in Table 8.

Table 8: Adsorption capacity at different adsorbent dosages (at 400 rpm)

Dosage (g/L)	% Removal	Final concentration (ppm)	Adsorption capacity (mg/g)
2	59.14	20.45	14.77
4	78.314	10.85	9.78
5	92.365	3.70	9.26
6	94.67	2.665	7.88

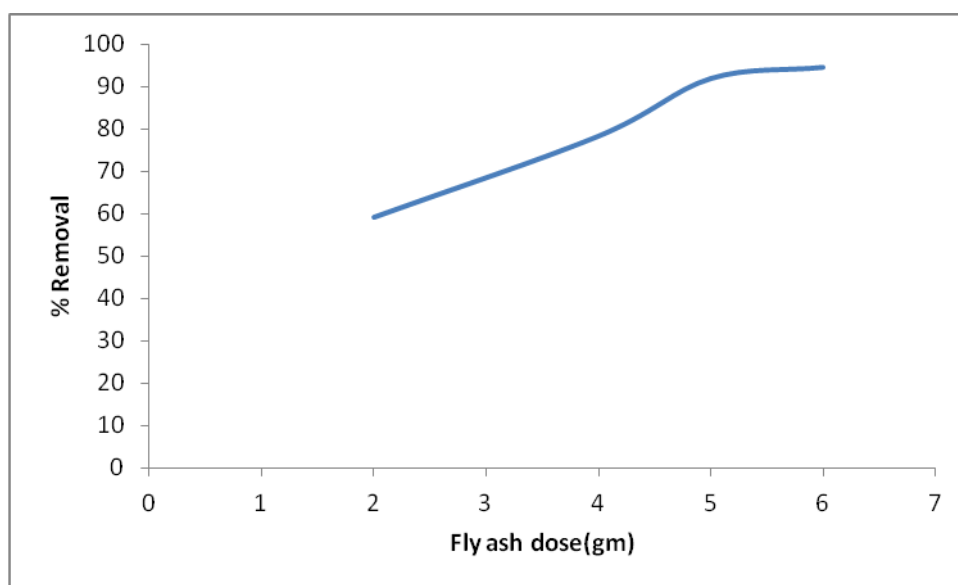


Figure 10: Effect of adsorbent dose on percentage removal of phenol

A plot of phenol percentage removal versus fly ash concentration yielded a non-linear profile as shown in Figure 10. From this figure, it can be observed that the percentage removal increased with increasing the fly ash concentration up to 5 g/L and no significant improvement in the percentage removal values was observed beyond this value. Hence, the optimal fly ash concentration for the removal of phenol was chosen to be 5 g/L. Initially, rapid increase in the adsorption with the increase in the adsorbent dose can be attributed to a greater surface area and availability of more adsorption sites. After this critical dose (5 g/L), the extent of adsorption is increasingly slowed down due to the fact that although there is increasing number of active sites but there is shortage of adsorbate in the solution.

5.6.2.1 Effect of used fly ash

Fly ash after being filtered from batch experiments is then again tried for an experiment so as to check whether fly ash can provide us with some significant results. It was observed in Table 9 that under similar conditions the percentage removal decreased exponentially mainly due to the absence of vacant sites necessary for adsorption. Figure 11 shows that active sites gets reduced and large clusters are formed which did not take part in further removal.

Table 9: Adsorption capacity of used fly ash

Dosage (gm)	% Removal	Final concentration (ppm)	Adsorption capacity (mg/g)
5	14	43	1.4

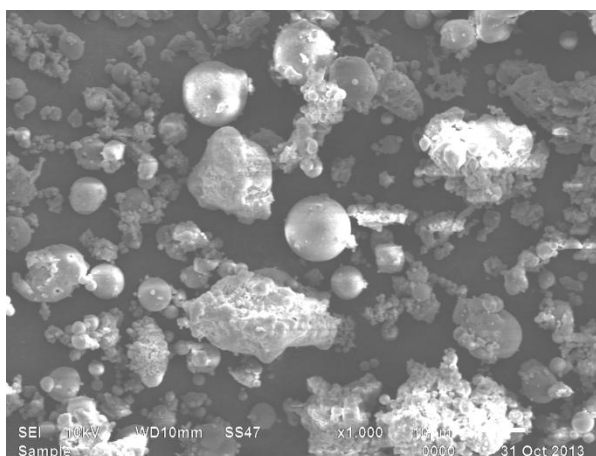


Figure 11: SEM image of the used/spent fly ash

5.6.3 Effect of solution pH

To study the effect of solution pH on the percentage phenol removal, adsorption experiments were conducted at various pH values between 4 and 12 for 2 hours at 400 rpm. The values of percentage phenol removal for various pH values are presented in Table 10 and the corresponding plot of phenol percentage removal versus pH is shown in Figure 12.

Table 10: Effect of solution pH on adsorption capacity

pH	Final concentration (ppm)	% Removal	Adsorption capacity(mg/g)
4	38.85	22.354	2.23
6	10.1	79.8125	7.98
7	7.5	85.147	8.51
8	14.55	70.985	7.09
10	26.15	47.741	4.77
12.	32.7	34.659	3.46

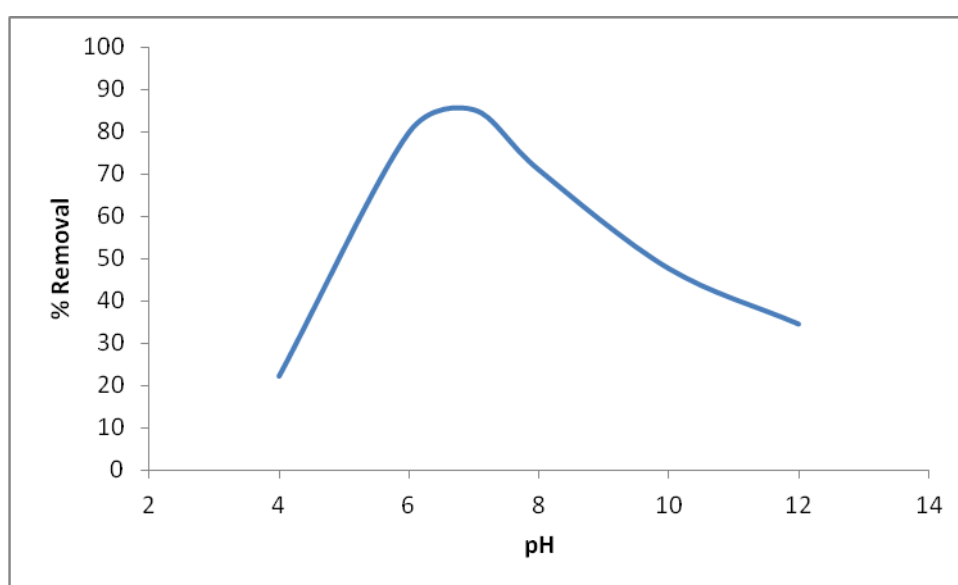


Figure 12: Effect of solution pH on phenol removal

Figure 12 shows that at low pH values percentage removals were very low whereas at higher pH values also percentage removal was not very high. This may be due to the presence of H^+ ions. These ions suppress the ionization of phenol and hence its uptake on adsorbent is reduced. At higher pH phenol forms salts that readily ionize leaving the negative charge on the phenolic group. At the same time OH^- ions on the adsorbent prevents the binding of ions that leads to low phenol adsorption.

5.6.4 Effect of phenol concentration

To study the effect of initial phenol concentration on the percentage removal, adsorption experiments were conducted at various phenol concentration values between 20 and 100 mg/L. The values of phenol percentage removal at various phenol

concentrations are presented in Table 11. Corresponding plot of percentage phenol removal versus initial phenol concentration is shown in Figure 13.

Table 11: Effect of phenol concentration on adsorption capacity

Concentration (ppm)	Final concentration (ppm)	% Removal	Adsorption capacity(mg/g)
20	0.02	99.96	3.99
40	1.92	95.23	7.61
50	4.0	92.0	9.2
60	7.11	88.14	10.57
80	15.88	80.14	12.82
100	27.86	72.14	14.42

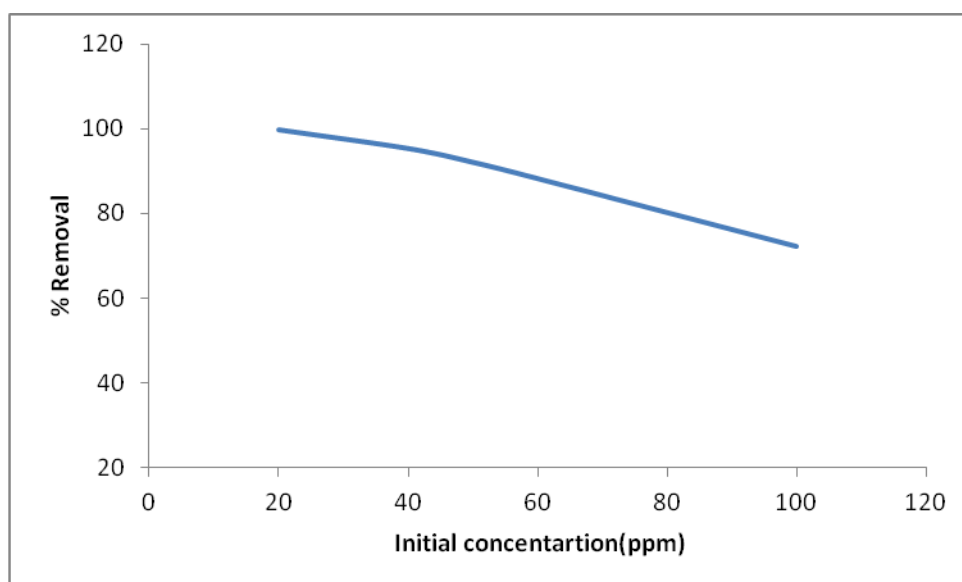


Figure 13: Effect of phenol concentration on percentage removal

From the above figure, it can be observed that the percentage removal decreases with increasing the initial phenol concentration. This indicates that the adsorption process is more effective at low concentrations of the phenol solution.

5.6.5 Effect of Temperature

To study the effect of temperature on the percentage removal of phenol, adsorption experiments were conducted at four different temperatures (27, 37, 47 and 57°C). The

values of percentage removal of phenol at different temperatures are presented in Table 12 and the corresponding plot of percentage removal of phenol versus temperature is shown in Figure 14.

Table 12: Effect of temperature on adsorption capacity

Temperature (°C)	Final concentration (ppm)	% Removal	Adsorption capacity(mg/g)
27	4.4	91.25	9.12
37	9.92	80.15	8.01
47	15.84	68.32	6.82
57	29.89	40.21	4.02

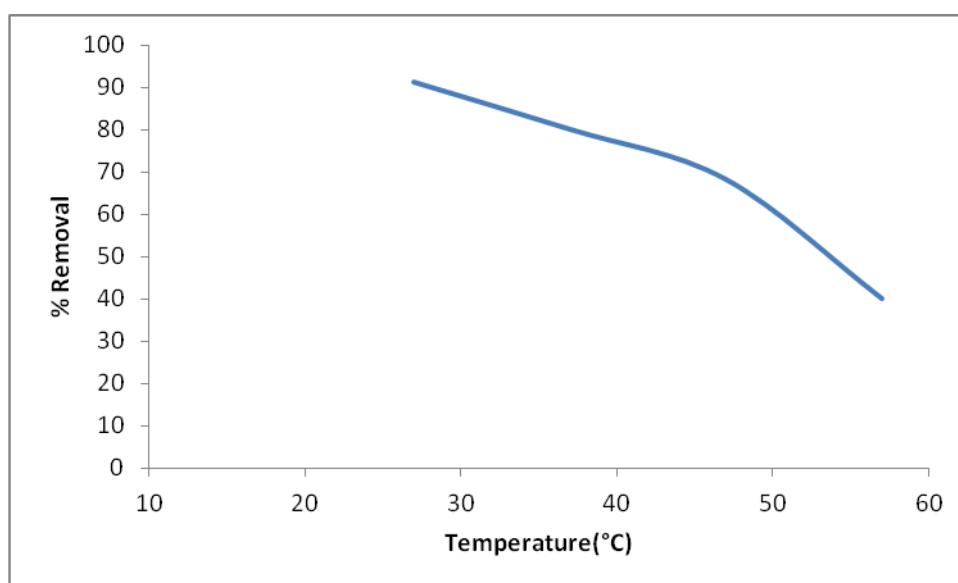


Figure 14: Effect of temperature on phenol removal

From the above figure, it can be observed that the percentage removal decreases with increasing the temperature. This indicates that adsorption is favoured at lower temperatures and desorption takes place at higher temperatures due to the fact that adsorption is exothermic in nature.

5.7 Thermodynamic, Kinetic and Equilibrium studies

5.7.1 Thermodynamics of adsorption

The thermodynamic parameters, such as the changes in the Gibbs free energy (ΔG°), enthalpy (ΔH°) and entropy (ΔS°) of adsorption process are estimated from the following correlations Equations (4) and (5).

The change in standard free energy (ΔG°) at various temperatures can be estimated as follows.

$$\Delta G^\circ = -RT \ln K_d = -RT \ln (q_e/c_e) \quad (4)$$

Here, R is the universal gas constant ($8.314 \text{ J mol}^{-1} \text{ K}^{-1}$), and T is the temperature in Kelvin (K). The calculated values of ΔG° are shown in Table 5.9. The relation among the thermodynamic parameters mentioned above is given by the following equation.

$$\Delta G^\circ = \Delta H^\circ - T\Delta S^\circ \quad (5)$$

Table 13: Values of Gibbs free energy (ΔG°) at different temperatures

Temperature (K)	ΔG°
300	1812.45
310	1872.64
320	1922.74
330	1991.86

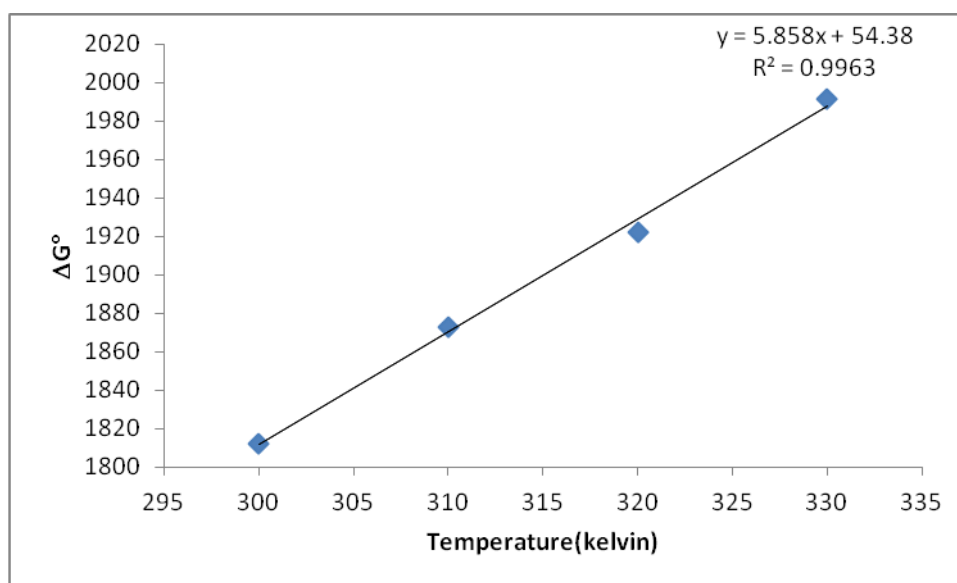


Figure 15: Plot of ΔG° versus temperature

A plot of ΔG° versus T, (Figure 15) yields a straight line with the slope of ΔS° and intercept of ΔH° . The values of ΔG° obtained using at the temperatures 300, 310, 320 and 330 K for phenol are 6.04, 6.12, 6.008 and 6.03 kJ/mol respectively. The values of changes in enthalpy (ΔH°) and entropy (ΔS°) during the adsorption process determined from the slope and intercept of Figure 15 are -5.85 kJ/mol and -54.38 J/mol K^{-1} respectively. The negative values indicate that the adsorption process considered here is exothermic in nature and hence lower temperatures are favoured.

5.7.2 Adsorption kinetics

Various kinetic models proposed to examine the controlling mechanism of adsorption process are a pseudo-first-order kinetic model, a pseudo-second-order kinetic model, and an intra-particle diffusion model. These three models are studied to find the best fitting model for the adsorption of dye on fly ash surface.

5.7.2.1 Pseudo first order kinetics

This model assumes that the rate of solute uptake is directly proportional to the concentration difference of the solute from the equilibrium saturation concentration on the adsorbent. The form of rate equation for a pseudo first-order kinetic model is as follows.

$$(dq_t/dt)=k_1(q_e-q_t) \quad (6)$$

Here, q_t (mg/g) is the amount of phenol adsorbed after time 't' (min), q_e (mg/g) is the equilibrium phenol adsorption capacity and k_1 (min^{-1}) is the pseudo first-order rate constant. The integration of equation with the initial condition $q_t = 0$ at $t = 0$ gives the following equation.

$$-\ln(1-q_t/q_e)=k_1t \quad (7)$$

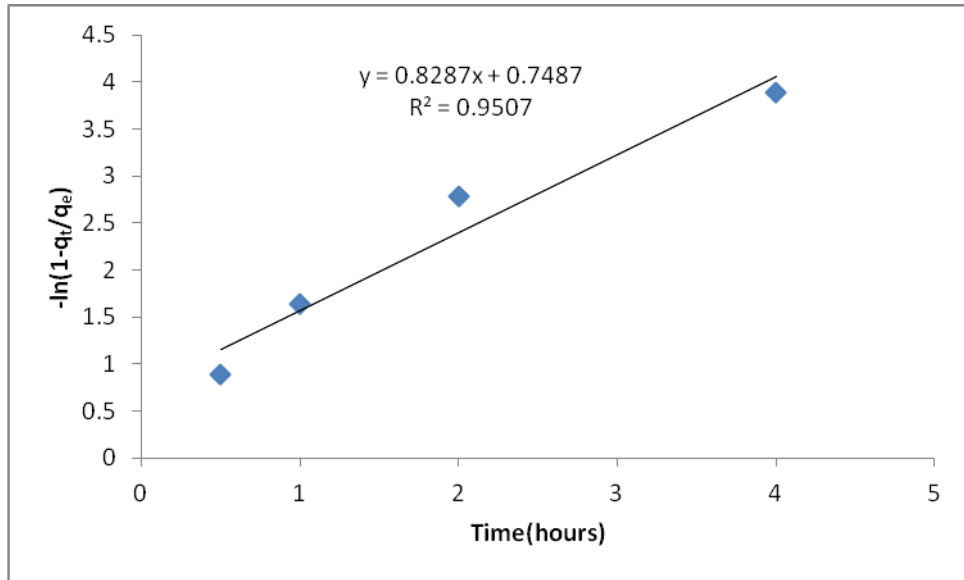


Figure 16: Pseudo first order kinetic model for adsorption of phenol on fly ash

The slope of a straight line fit to the data of $-\ln(1-q_t/q_e)$ versus time gives the value of the pseudo first-order rate constant, k_1 . The experimental data was found to be fitting well with the pseudo first-order model. The value of the pseudo first order rate constant, k_1 as obtained from the linear curve fitting is 0.8287 min^{-1} for phenol. The value of q_e as obtained from the regression analysis (9.81 mg/g) for phenol is very much close to the experimental value (9.8 mg/g). This indicates that the pseudo first-order kinetic model can adequately represent the phenol–fly ash system under consideration.

5.7.2.2 Pseudo second-order kinetics

This model interprets that the rate of solute uptake is directly proportional to the square of the concentration difference of the solute from the equilibrium saturation concentration on the adsorbent. The form of rate equation for a pseudo second-order kinetic model is as follows.

$$dq_t/dt = k_2(q_e - q_t)^2 \quad (8)$$

Here, $k_2 \text{ (g.mg}^{-1}.\text{min}^{-1})$ is the pseudo second-order rate constant. The integration of equation with the initial condition $q_t = 0$ at $t = 0$ gives the following expression.

$$t/q_t = (1/q_e^2 k_2) + (t/q_e) \quad (9)$$

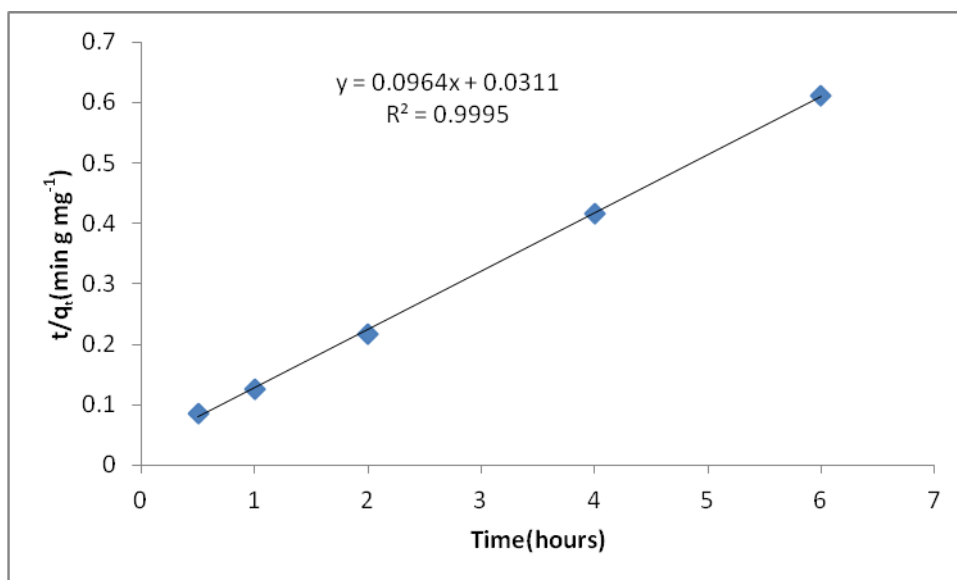


Figure 17: Pseudo second order kinetic model for the adsorption of phenol on fly ash

The values of q_e and k_2 can be obtained from the slope and intercept of a straight line fit to the data of t/q_t versus t (as shown in Figure 17). The slope and intercept obtained from the graphical analysis of phenol plot are 0.0964 and 0.0311. The values of q_e and k_2 thus obtained are 4.72 mg/g and 0.612 g.mg⁻¹.min⁻¹ respectively. The regression coefficient value of q_e (4.72 mg/g) it is not matching with experimental value (9.8 mg/g). Therefore, the pseudo second-order kinetic model is not appropriate for the phenol–fly ash system considered in this study.

5.7.2.3 Intra particle diffusion

This model considers the bulk diffusion, film diffusion, pore diffusion in addition to the adsorption phenomenon. The form of rate equation for the intra-particle diffusion model is as follows.

$$q_t = k_i t^{0.5} + C_i \quad (10)$$

Here, k_i (mg/g.min⁻¹) is the intra-particle diffusion rate constant and C_i (mg/g) is the intercept, which corresponds to the boundary layer thickness. The values of k_i and C_i can be determined directly as the slope and intercept of the linear plot of q_t versus $t^{0.5}$. The values of k_i and C_i obtained from the graph are 2.058 mg/g.min⁻¹ and 5.3479 mg/g respectively for phenol.

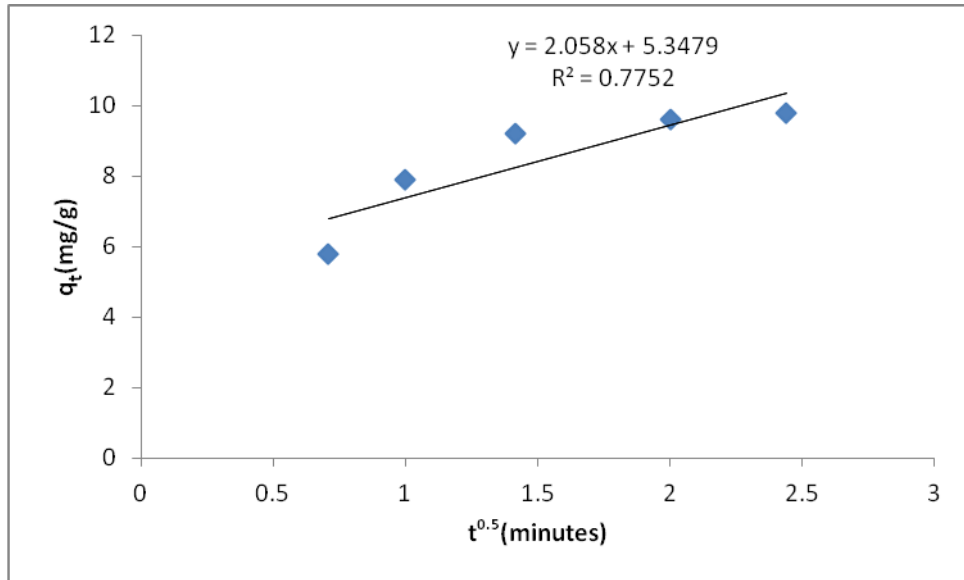


Figure 18: Intra particle diffusion model for the adsorption of phenol on fly ash

5.7.2.4 Equilibrium adsorption isotherm

Adsorption isotherms describe the nature of interaction between the adsorbent and the adsorbate molecules at equilibrium. The two most common types of adsorption isotherms are Langmuir and Freundlich isotherms. The parameters of these equilibrium isotherms are useful in the optimum design of adsorption systems. The Langmuir isotherm simply assumes that there is a homogeneous distribution of active sites (binding sites) on the surface of the adsorbent, which adsorb a single molecular layer of adsorbate molecules with no interaction between the adsorbed molecules. The Langmuir isotherm equation is given by

$$q_e = \frac{Q_m K_L C_e}{1 + K_L C_e} \quad (11)$$

Where, C_e (mg/L) and q_e (mg/g) are the liquid phase concentration and solid phase concentration of adsorbate at equilibrium, and Q_m (mg/g) corresponds to the maximum adsorption capacity of the adsorbent where as K_L (L/mg) corresponds to the equilibrium adsorption constant of the Langmuir isotherm.

The linearized form of equation (12) is as follows.

$$C_e/q_e = (1/Q_m K_L) + (C_e/q_m) \quad (12)$$

The values of Q_m and K_L can be determined from the slope and intercept of a linear curve fit to the plot of C_e/q_e versus C_e (shown in Figure 19). Further, the equilibrium

adsorption intensity (R_L), which indicates the type of adsorption, is defined as follows.

$$R_L = 1 / (1 + K_L C_i) \quad (13)$$

Here, C_i is the initial dye concentration (mg/L) in the solution. For a favourable adsorption, $R_L < 1$; for a linear adsorption, $R_L = 1$; and for an unfavourable adsorption, $R_L > 1$. A plot of R_L versus C_i is shown in Figure 20. From this figure, it can be observed that the adsorption process is more favorable at higher concentrations of phenol solution.

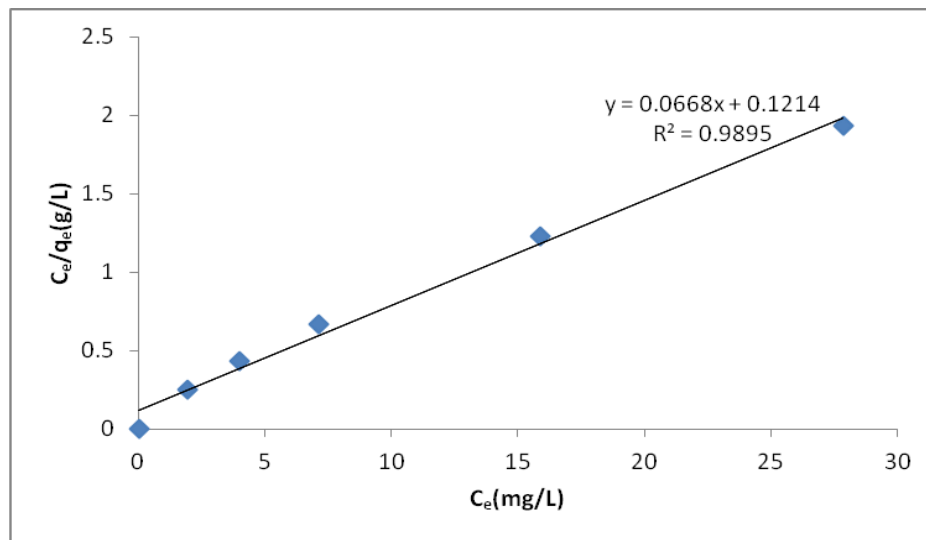


Figure 19: Plot of C_e versus C_e/q_e for the estimation of Langmuir isotherm constants

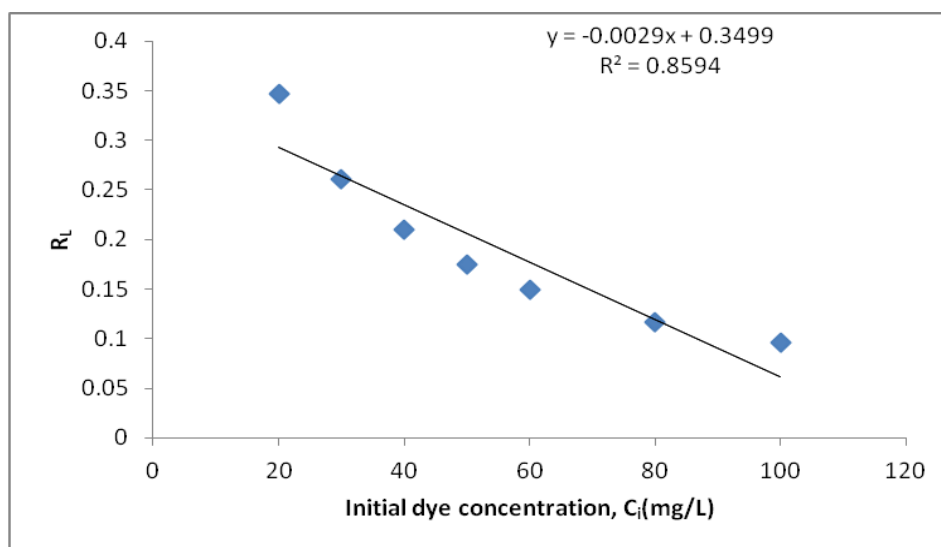


Figure 20: Variation of equilibrium adsorption intensity (R_L) with initial phenol concentration (C_i)

The Freundlich isotherm model is an exponential equation, which applies to heterogeneous systems with interaction between adsorbed molecules and is not restricted to the formation of a monolayer. This model assumes that as the adsorbate concentration increases, the concentration of the adsorbate on the adsorbent surface also increases and correspondingly that sorption energy exponentially decreases on completion of the sorption centers of an adsorbent. The well-known expression for the Freundlich model is as follows.

Where, ' K_F ' is the Freundlich constant ($\text{mg/g} \cdot (\text{mg/L})^{-n}$) related to the bonding energy, and n is the heterogeneity factor (exponent). Here, ' n ' is a measure of the deviation from linearity of the adsorption and indicates the degree of non-linearity between the solution concentration and the adsorption rate. A power-law model curve fit to the data of q_e versus C_e could yield the values of K_F and n . The isotherm plot for the phenol–fly ash system is shown in Figure 21. From this figure, it can be observed that the equilibrium adsorption between phenol and fly ash can better be represented by Freundlich isotherm model rather than Langmuir isotherm.

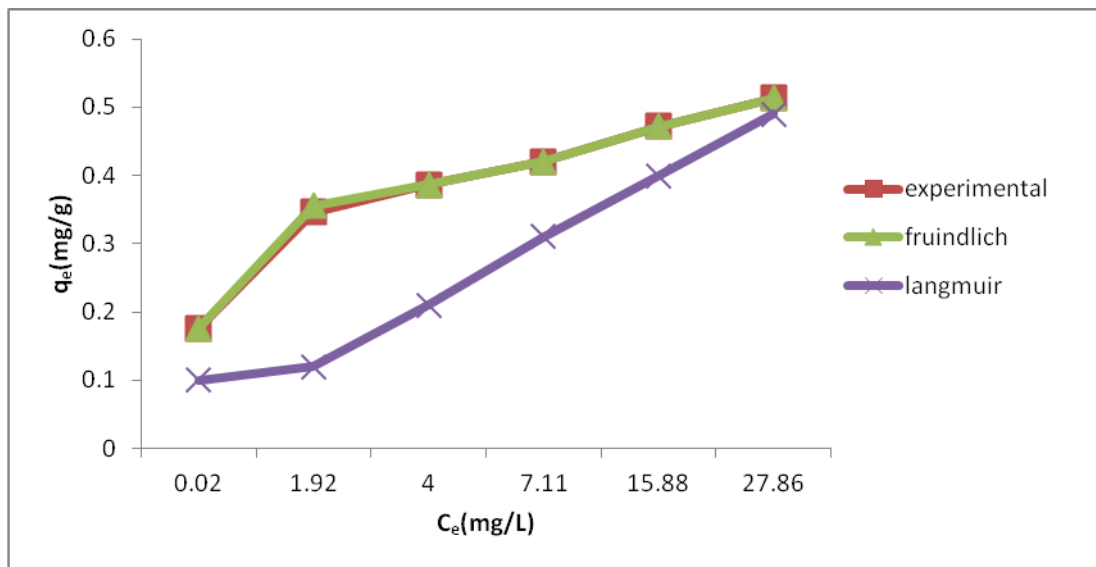


Figure 21: Equilibrium isotherms for the adsorption of phenol on fly ash

Table 14: Equilibrium parameters for Langmuir and Fruindlich adsorption isotherms

Langmuir isotherm		Fruindlich isotherm	
Parameter	Value	Parameter	Value
Q_m	0.066	K_F	0.3159
K_L	0.121	$1/n$	0.147
R^2	0.9895	R^2	0.9967

The trend observed in the experimental data is very close to the Fruindlich isotherm but it is deviating considerably from the Langmuir isotherm. This indicates that the adsorption process is of multi-layer type with some interaction among the adsorbed molecules. The evaluated model parameters for both Langmuir and Fruindlich adsorption isotherms are presented in Table 14. Corresponding values of correlation coefficients (R^2) are also shown in the table.

The washed and dried fly ash has been successfully applied for the adsorptive removal of phenol from its aqueous solution. The following conclusions have been derived from the experimental analysis carried out so far.

- The washed and dried fly ash is found to be more effective than the synthetic adsorbent presented in the literatures.
- The optimum fly ash concentration obtained from the experimental studies is 5 g/L.
- λ_{\max} for phenol solution was 293 nm. The calibration curve for phenol was also observed.
- Optimum adsorption time was 2 hrs for the phenol.
- Optimum pH value was 7 for phenol removal using fly ash.
- Optimal stirrer speeds were found to be 400 rpm using fly ash for the removal of phenol.
- Percentage removal decreases with increasing the initial phenol concentration.
- Percentage removal increases with increasing the adsorption time.
- Adsorption process is exothermic and is favoured at low temperatures.
- Experimental data matches well with the pseudo-first-order kinetics.
- Experimental data matches well with the Freundlich isotherm.

The most important observation in this work is that the percentage removal increased with increasing the fly ash concentration significantly and reached a value as high as 72% at lower concentrations (up to 100 mg/L) of phenol.

Work done so far includes the study of effect of various parameters on the removal of phenol. However there is a lot of scope for further research in this area. Some of the objectives that can be studied in future are as follows.

1. Studying the performance of unburnt carbon extracted from fly ash for the removal of phenol and other phenolic compounds used in industry.
2. Using the washed fly ash for industrial wastewater treatment in continuous mode (fixed bed or fluidized bed studies).
3. Removal of heavy metals from water by adsorption with the washed fly ash.

References

- Anna, W., K., Roman, G., Szafran and Szymon, M., 2011, Biosorption of heavy metals from aqueous solutions onto peanut shell as a low-cost biosorbent, *Desalination*, 265, 126–134.
- Abburi, K., 2003, Adsorption of phenol and p-chlorophenol from their single and bisolute aqueous solutions on Amberlite XAD-16 resin. *Journal of Hazard Materials*, B105, 143–156
- Adak, A., Pal, A., Bandyopadhyay, M., 2006. Removal of phenol from water environment by surfactant-modified alumina through adsolubilization. *Colloids Surfactants Physicochemical*, 277, 63–68
- Celik, O., Damci, E., 2008. Characterization of fly ash. *Indian journal of engineering and material sciences*, 15, 431-40
- Chan, W., Chun, F., 1998. Adsorption /ion-exchange behaviour between a water insoluble cationic starch and 2-Chlorophenol in aqueous solutions. *Journal of Applied Polymer Science*, 67, 1085–1092
- Calace, N., Nardi, E., Petronio, B.M., Pietroletti, M., 2002. Adsorption of phenols by paper mill sludge. *Environmental Pollution*, 118, 315–324.
- Cornelia, Pacurariu, Georgette, Adriana M., 2013. Adsorption of phenols & chlorophenols from aqueous solutions on poly functionalized materials. *Chemical Engineering Journal*, 222, 218–227
- Crini, E., Nagri, M.D., 2006. Adsorption of phenol onto peanut shell. *Environmental Pollution*, 165,267-291.
- Erso, A., Denizli, A., Sener, I., Atılır, A., Diltemiz, S., Say, R., 2004. Removal of phenolic compounds with nitrophenol-imprinted polymer based on p-p and hydrogen-bonding interactions. *Separation Purification Technology*, 38, 173–179.
- Gonzalez-Serranoa, E., Corderoa, T., Rodriguez-Mirasola, J., Cotorueloa, L.,

- Rodriguez, J.J., 2004. Removal of water pollutants with activated carbons prepared from H₃PO₄ activation of lignin from kraft black liquors. *Water Research*, 38, 3043–3050.
- Goncharuk, M., Badekha, P., 2002. Removal of organic substances from aqueous solutions by reagent enhanced reverse osmosis. *Desalination*, 143:45–51.
- Gupta, A., Suhas, M., 2006. An overview of comparison of synthetic samples with natural samples. *Journal for Colloid Interface Science*, 154, 365-385.
- Jain, A.K., Gupta, V.K., Jain, S., Has, S., 2004. Removal of chlorophenols using industrial wastes. *Environmental Science Technology*, 38, 1195–1200.
- Juang, R.S., Lin, S.H., Tsao, K.H., 2002. Mechanism of sorption of phenols from aqueous solutions onto surfactant-modified montmorillonite. *Journal of Colloid Interface Science*, 254, 234–241.
- Koyama, O., Kamagat, Y., Nakamura, K., 1994. Degradation of chlorinated aromatics by Fenton Oxidation and methanogenic digester sludge. *Water Research*, 28, 895–899
- Mokrini, A., Ousse, D., Esplugas, S., 1997. Oxidation of aromatic compounds with UV radiation/ozone/ hydrogen peroxide. *Water Science Technology*, 35, 95–102
- Mukherjee, S., Kumar, S.A., Misra, K., Fan, M., 2007. Removal of phenols from water environment by activated carbon, bagasse ash and wood charcoal. *Chemical Engineering Journal*, 129, 133–142
- Maria, D., Otto, F., Nama G., 2006. Removal of phenol by maize waste. *Chemical Engineering Journal*, 201,196-205
- Muthamil,E.,Sharma K., 2012. Removal of aqueous phenol by PGF (pongamia glabra flower). *Journal of Environmental Management*, 90, 195-209.
- Otero, M., Rozada, F., Calvo, L.F., Garcia, A.I., Moran, A., 2003. Elimination of organic water pollutants using adsorbents obtained from sewage sludge. *Dyes Pigmentation*, 57, 55–65.

- Polcaro, A.M., Palmas, S., 1997. Electrochemical oxidation of Chlorophenols. *Engineering Chemical Research*, 36, 1791–1798
- Roostaei, N., Tezel, F.H., 2004. Removal of phenol from aqueous solutions by adsorption. *Journal for Environmental Management*, 70, 157–164.
- Radhika, M., Palanivelu, K., 2006. Adsorptive removal of chlorophenols from aqueous solution by low cost adsorbent-kinetics and isotherm analysis. *Journal of Hazardous Materials*, 138, 116–124.
- Sathishkumar, M., Binupriya, A.R., Kavitha, D., Yun, S.E., 2007. Kinetic and isothermal studies on liquid-phase adsorption of 2, 4-dichlorophenol by palm pith carbon. *Bioresource Technology*, 98, 866–873.
- Srivastava, V.C., Swamy, M.M., Mall, I.D., Prasad, B., Mishra, I.M., 2006. Adsorptive removal of phenol by bagasse fly ash and activated carbon: equilibrium, kinetics and thermodynamics. *Colloids Surfactants*, 272, 89–104.
- Sarkar, M., Acharya, P.K., 2006. Use of fly ash for the removal of phenol and its analogues from contaminated water. *Waste Management*, 26, 559–570.
- Lin, S., 2008. Removal of phenol using zeolite. *Journal of colloid interface science*, 304, 206-209.
- Tor, A., Cengeloglu, Y., Aydin, M.E., Ersoz, M., 2006. Removal of phenol from aqueous phase by using neutralized red mud. *Journal for Colloid Interface Science*, 300, 498–503.
- Tarasevich, Y., 2001. Porous structure and adsorption properties of natural porous coal. *Colloids Surfactants*, 176, 267–272.
- Wang, H.L., Jiang, W.F., 2007. Adsorption of dinitrobutyl phenol from aqueous solutions by fly ash. *Industrial Engineering Chemical Research*, 46, 5405–5411.
- Yapar, S., Zbudak, V., Dias, A., Lopes, A., 2005. Effect of adsorbent concentration to the adsorption of phenol on hexadecyl trimethyl ammonium-bentonite. *Journal for Hazardous Materials*, 121, 135–139.